water

MDPI

Article

Spatiotemporal Characteristics of Meteorological Drought and Wetness Events across the Coastal Savannah Agroecological Zone of Ghana

Johnson Ankrah [1,*], Ana Monteiro [1,2,3] and Helena Madureira [1,3]

[1] Faculty of Arts and Humanities, Geography Department, University of Porto, Via Panorâmica Edgar Cardoso, 4150-564 Porto, Portugal
[2] Research Centre for Territory, Transport and Environment (CITTA), Rua Dr. Roberto Frias, s/n, 4200-465 Porto, Portugal
[3] Centre of Studies in Geography and Spatial Planning (CEGOT), Geography Department, University of Porto, Via Panorâmica Edgar Cardoso, 4150-564 Porto, Portugal
* Correspondence: up201701629@edu.letras.up.pt

Abstract: Drought and wetness events have become common due to global warming, warranting the need for continuous analysis and monitoring of drought and wet events to safeguard people's livelihoods. In this study, the Standardized Precipitation Evapotranspiration Index (SPEI) was utilized to analyze the spatiotemporal characteristics of drought and wetness events in the coastal Savannah agroecological zone from 1981 to 2021. Climate data from 14 locations across the zone were used to characterize drought and wetness events at the 3 and 12 month timescales. Except for September 1995 and November 2002, when changepoints occurred, the results revealed the homogeneous nature of temperature and rainfall in the zone. More drought events were observed in the dry and minor seasons, while the wet season had more wetness events under both the SPEI-3 and SPEI-12 timescales. The results also showed that, while moderate-to-severe drought events were common for most years, extreme drought events were more typical in the 1980s and 1990s than in the 2000s under both the SPEI-3 and SPEI-12. Furthermore, the 2000s saw more moderate-to-severe wetness events than the 1980s and 1990s, while the greatest number of extreme wetness events occurred in 1987, followed by 1997 and 2021 under the SPEI-3, and a few moderate-to-extreme wetness events occurred in 1987, 1991, 1997–1998, 2012–2013, 2018, and 2020–2021 under the SPEI-12. Under the SPEI-12, only extreme drought events showed a significant positive trend with a small magnitude of change. On the spatial scale, drought and wetness events occurred more frequently in the Central and Volta regions than in the Greater Accra region; however, the intensity and duration of the events were stronger and lasted longer in the Greater Accra and Central regions than in the Volta region. The regular monitoring of drought and wetness events is required to protect the livelihoods of people in the zone.

Keywords: drought; wetness events; SPEI; spatial variation; drought frequency; drought intensity; Ghana

Citation: Ankrah, J.; Monteiro, A.; Madureira, H. Spatiotemporal Characteristics of Meteorological Drought and Wetness Events across the Coastal Savannah Agroecological Zone of Ghana. *Water* **2023**, *15*, 211. https://doi.org/10.3390/w15010211

Academic Editor: Luis Gimeno

Received: 2 December 2022
Revised: 29 December 2022
Accepted: 30 December 2022
Published: 3 January 2023

1. Introduction

Drought continues to be one of the greatest natural disasters facing humanity [1] and has become more frequent in recent times due to global warming [2–4]. As a natural hazard, drought poses threats to agricultural, social, economic, and environmental systems, negatively affecting the livelihood opportunities of many people [5–8]. As has been reported by the International Disaster Database (EM-DAT), 432 natural disasters were recorded in the year 2021, including drought, which affected 101.8 million people with 10,492 deaths and economic damage worth 252 billion United State dollars [9]. In the West African region, the number of significant disasters that occurred from 2000 to 2010 (1975–2011) included flooding (133 (196)), drought (15 (59)), extreme temperatures (1 (3)), earthquakes (0 (1)),

mass movements of moisture (4 (3)), storms (12 (6)), volcanoes (0 (1)), wildfires (1 (5)), and dry landslides (0 (1)) [10].

Indeed, drought is intricate and considered one of the least-understood natural disasters [11]. There are spatial and temporal variations in the frequency, duration, and intensity of drought, as an extreme event [12]. These spatial and temporal variations in drought have given room for various definitions, making it difficult to derive a definite universal definition [12]. Kogan [13] highlighted the need for the identification and incorporation of area variations, such as physiological features, prevailing climatic conditions, economic development, and their effects on livelihoods, when defining and characterizing drought. Nonetheless, drought is inadequately defined and characterized at present, particularly in data-scarce areas, casting doubt on the relevance and appropriateness of relevant drought execution plans [12,14,15]. Drought occurs as a result of negative water imbalances caused by a prolonged lack of precipitation or excess evapotranspiration over a prolonged period [16,17]. Based on the above definition, four distinct types of drought can be recognized, namely, meteorological, agricultural, hydrological, and socio-economic [17–20]. Previous research studies, such as [6,7,12,19,21,22], have defined and explained the various types of droughts. Mishra and Singh [19] advocated for the addition of groundwater drought as a fifth type of drought. Meteorological drought, which is seen as an extreme climate event, plays a significant role in the other types of droughts [23,24].

Considering the intricate and challenging nature of drought characterization [25], there has been increasing interest in the development of appropriate drought indices for drought monitoring, assessment, and the creation of early warning systems [12,26]. As emphasized by Quiring and Ganesh [27], most of these indices use meteorological variables such as variations in precipitation. Such indices include the Drought Severity Index (PDSI) [21], the Standardized Precipitation Index (SPI) [16], and the Standardized Precipitation Evapotranspiration Index (SPEI) [15], among others. These drought indices have been used in numerous research studies [1,15,28–38]. Of course, numerous drought indices exist, as underlined by Liu et al. [39]. Heim et al. [12] classified the numerous drought indices into site-based and remote sensing-based ones. The remote sensing-based drought indices include those such as the Vegetation Condition Index (VCI) proposed by Kogan [13] and the Normalized Difference Water Index (NDWI) by Gao [40], among others. It should be noted that all of these indices have certain strengths and weaknesses.

In the context of global warming, the incidence of extreme events such as droughts and floods is projected to increase in many regions around the world [41]. Thus, significant efforts have been given towards understanding drought dynamics and related impacts, in the quest to develop mitigation measures [41–43]. Notwithstanding these efforts, drought evolution, duration, frequency, and intensity remain a challenge and are not well-realized, due to their intricacies in comparison to other natural disasters [44,45]. Many research studies have been carried out on droughts in many parts of the world in the context of global warming [41,42,46], as scientists wish to understand all the details; for example, in Africa [47–49], Asia [50–52], Australia [53–55], Europe [6,56,57], North America [2,58,59], and South America [60–62]. There has also been drought research at the global level (see, e.g., [42,46,63–65]).

Drought is an intrinsic attribute of the West African climate and is recognized as one of the major causes of associated economic difficulties, migration, and mortality [66]. For instance, the extreme drought events in the West African regions in the 1970s and 1980s caused water shortages for both social and agricultural use [66]. This caused famine, which led to the deaths of between 100,000 and 250,000 people, and about 3.5 million livestock worth $400 million perished [67]. In Ghana, the incidence of extreme drought caused a series of bush fires that led to the loss of properties, human lives, and farmlands [68].

Extreme events such as droughts and floods have increased in Ghana in recent decades, making the country vulnerable [69,70]. Many research studies have been performed to analyze drought in Ghana. For instance, Kasei et al. [71] utilized the SPI to investigate the temporal characteristics of meteorological drought in the Volta basin, in order to

provide support for water resource management. Similarly, Ndehedehe et al. [72] used the SPI, Standardized Runoff Index (SRI), and Standardized Soil moisture Index (SSI) to analyze the spatiotemporal patterns of drought in the Volta river basin for hydrological monitoring. Likewise, Nyatuame and Adodzo [73] employed the SPI to characterize the magnitude, duration, frequency, commencement, and termination of drought and flood in the Tordzie watershed, and they highlighted the possible effects on agriculture and management of water resources. Additionally, Oguntunde et al. [74] utilized the SPI, SPEI, and the Standardized Runoff Index (SRI) to examine drought characteristics in the Volta river basin, and they underlined the impacts on agriculture, water resources, and energy supply. Dovie and Kasei [75] also employed the SPI to highlight the increased drought and flood influence on groundwater recharge and irrigation in the White Volta river basin. In addition, Akurugu et al. [76] studied the groundwater resources in the Densu river basin in south-western coastal Ghana, and they concluded that the basin's recharge rate is at risk of decreasing due to the impacts of climate change and urbanization. Furthermore, Nasirudeen et al. [77] used the SPI and Reconnaissance Drought Index (RDI) to analyze drought patterns in the Tano river basin and found that drought had a negative impact on agricultural production and water supply along the river. Addi et al. [78] used the SPI to study large-scale droughts along the coast of Ghana, in order to obtain better information for early warming and disaster risk management.

The research studies mentioned above were predominantly concentrated in the Volta river basin and the Savannah agroecological zone, with few conducted in equally important locations, such as the coastal areas. Addi et al. [78] attempted to investigate meteorological drought in coastal Ghana; however, they made no attempt to analyze the spatial variations and the incidence of drought and wetness events. Furthermore, most of the studies did not attempt to characterize the frequency, duration, and intensity of the drought and wet events. A detailed drought and wetness event analysis in coastal Ghana is crucial for recognizing and comprehending the complexities associated with these events during the current phase of global warming, which remains challenging.

In this study, we employed the widely applied SPEI [15] to analyze the spatiotemporal characteristics of drought and wetness events based on frequency, duration, and intensity in the coastal Savannah agroecological zone in Ghana in 1981–2021. In addition, we performed a homogeneity test on the temperature and rainfall time-series data and analyzed the monthly variations in drought and wetness events in the zone, as well as the temporal evolution and trends in drought and wetness events in the zone. The findings of the present study provide important insights regarding the analysis of drought and wetness events, which can support the decision-making process of smallholder farmers and water resource managers in the coastal Savannah agroecological zone of Ghana.

2. Materials and Methods

2.1. Study Area

Ghana is in West Africa, with a latitude of 4°44′ N to 11°11′ N and a longitude of 3°11′ W to 1°11′ E [79]. Ghana has a tropical climate, with both dry and wet seasons, which is strongly influenced by the West African Monsoon (WAM) and the Intertropical Discontinuity (ITD) [78]. Ghana is divided into six major agroecological zones, based on climate, vegetation, and soil, as follows: Coastal Savannah, Rain Forest, Deciduous Forest, Transition Zone, Guinea Savannah, and Sudan Savannah [79].

This study focuses on the coastal Savannah agroecological zone (Figure 1). The elevation of the coastal Savannah agroecological zone ranges from the lowest point of −3.8 m on the coast to the highest point of 641.2 m inland (Figure 1a). This zone is the driest in the country [80,81], with a maximum and minimum mean annual temperature of 27.9 °C and 26.6 °C, respectively (Figure 1b). Despite having a bimodal rainfall regime, it is the zone that receives the lowest rainfall [82,83]. The average annual rainfall ranges from a low of 978.4 mm to a high of 1339.9 mm (Figure 1c). The major rainfall season in the zone begins from April to July, and the minor season occurs from September to early November,

while the dry season commences from late November to March [84]. Major towns in this zone (Figure 1a) include Elmina, Cape Coast, Moree, Saltpond, Apam, Winneba, Bortianor, Accra, Tema, Prampram, Ada Foah, Anloga, Keta, and Denu. The zone's primary economic activities include fishing, agriculture, and trading [78].

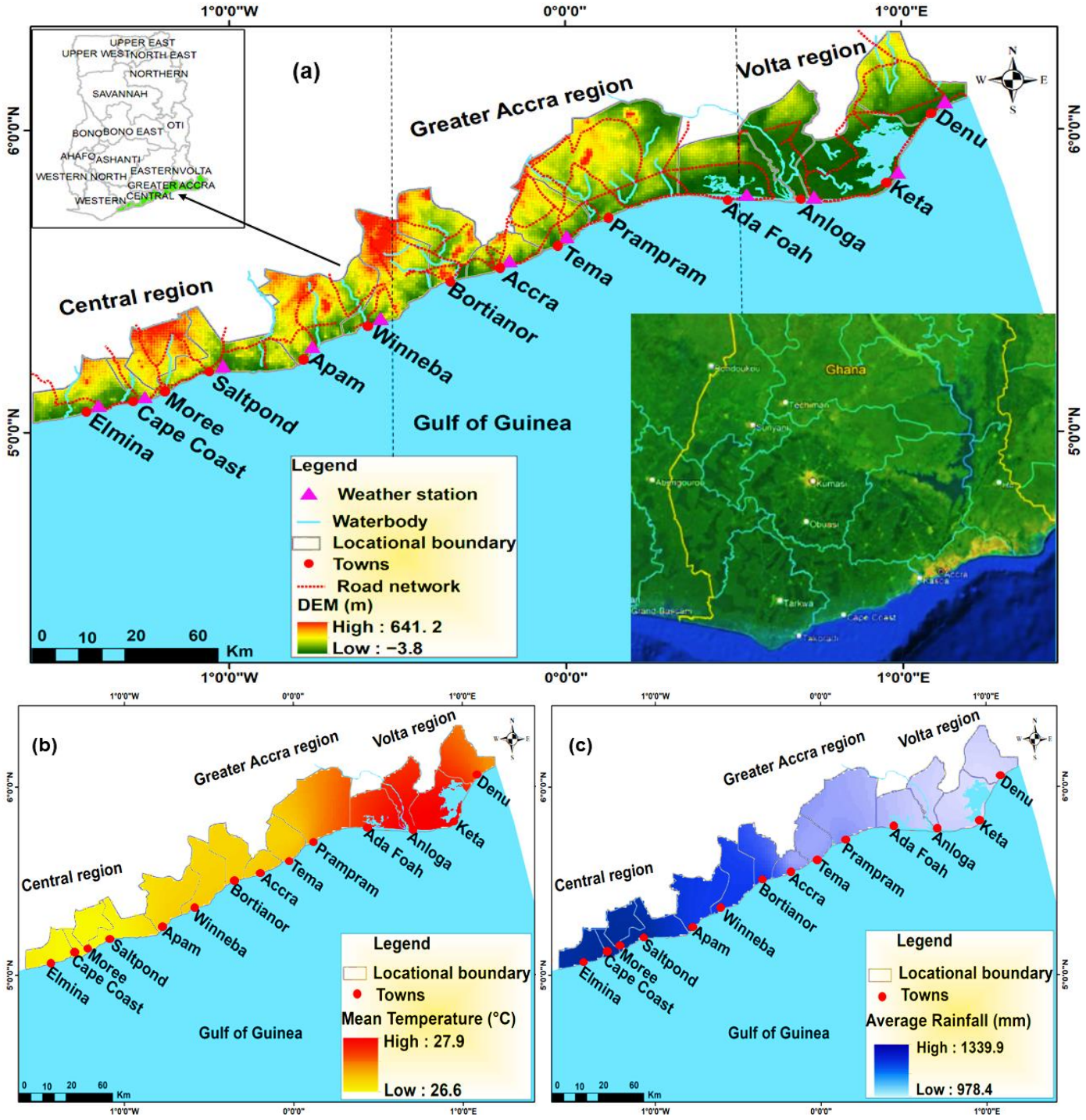

Figure 1. Map showing the location of the coastal Savannah agroecological zone, elevation, major towns, and measurement stations (**a**); average annual rainfall (from 1981 to 2021) (**b**); mean annual temperature (from 1981 to 2021) (**c**).

2.2. Data Sources and Quality Control

Monthly climatological data for 14 locations (Figure 1b) from 1981 to 2021 were obtained, in order to characterize drought and wet events in the Coastal Savannah agroecological zone. The data utilized included monthly rainfall and maximum and minimum temperatures acquired from the Ghana Meteorological Agency (GMet) and the National Aeronautics and Space Administration/Prediction of Worldwide Energy Resources (NASA/POWER) [85]. From GMet, we obtained data for eleven synoptic stations—Elmina, Cape Coast, Saltpond, Apam, Winneba, Accra, Tema, Ada Foah, Anloga, Keta, and Denu—whereas those for Moree, Bortianor, and Prampram were acquired from NASA/POWER.

GMet is the representative agency for climatological data provision in Ghana, while NASA/POWER is a satellite-based data set that provides global weather and agroclimatology data at 1° latitude and longitude resolution [86]. NASA/POWER satellite data have been widely utilized [86–88] and are considered suitable and dependable, especially for filling data gaps in data-scarce regions such as developing countries [86].

The R-Instat (version 0.70) software [89] was used to check for missing gaps in the rainfall and temperature data sets from the eleven synoptic stations. Here, the missing gaps in each data set were less than 2%. Following the advice of Monteiro et al. [86], the NASA/POWER satellite data were used to fill in these gaps.

2.3. Methods

2.3.1. Homogeneity Tests of the Observed Temperature and Rainfall Time-Series Data

In this study, we performed three homogeneity tests to detect shifts or breaks (inhomogeneities) in the observed monthly temperature and rainfall time-series data. These tests included the Pettitt test [90], the Buishand range test [91], and the Standard Normal Homogeneity Test (SNHT) [92]. These tests are highly recommended for detecting homogeneity in a given time-series data set [93,94]. The tests can recognize shifts in the time-series to detect changepoints and their corresponding years of change [94]. Furthermore, the Pettitt test and the Buishand range test can identify changepoints in the middle of the time-series, while the beginning and end of the time-series were the cases assessed by the SNHT [93,94]. The Pettitt test is a non-parametric test and does not require the assumption of a normally distributed time-series; the opposite is true for the Buishand range test and the SNHT [93–95].

Criteria for Homogeneity Analysis

In this study, we used the method of Winingaard et al. [93] to detect changepoints in climate variables. A series is said to be homogeneous (HG) if the calculated *p*-value of all three tests is greater than the significance level alpha of 0.05. If the estimated *p*-value of at least two of the three tests is less than the significance level alpha of 0.05 and at least two of the three tests have the same year of change, there is considered to be a changepoint (CP) in the series. In addition, if each of the three tests identifies a changepoint in different years, the series is considered uncertain (U). This method was successfully utilized in the earlier studies of Yildirim and Rahman [94] and Jaiswal et al. [95].

2.3.2. Computation of SPEI

As described earlier, the SPEI uses the climatic water balance, which is calculated from the difference between precipitation and potential evapotranspiration (PET) [15]. The SPEI, thus, has the capability to portray the variations in drought and wet conditions through changes in water supply and demand [47]. The SPEI was computed using the SPEI package in R. A detailed computation procedure for the SPEI has been provided by Vincente-Serrano et al. [15], as follows:

$$D_i = P_i - \mathrm{PET}_i, \quad (1)$$

where D_i is the moisture deficit in millimeters for month i, P_i denotes the precipitation in millimeters for month i, and PET_i denotes the potential evapotranspiration in millimeters for month i. The Hargreaves method [96] was used to compute the PET, considering the usage of only maximum and minimum temperatures [97].

The estimated D_i values were summarized at different timescales. The difference $D^k_{i,j}$ between a particular month j and year i was determined according to the selected timescale k. As indicated in the study of Vincente-Serrano et al. [15], the accumulated difference, for example, for one month in a given year i with a 12 month timescale, is estimated as follows:

$$X^k_{i,j} = \sum_{l=13-k+j}^{12} D_{i-1,l} + \sum_{l=1}^{j} D_{i,l}, \text{ if } j < k \text{ and} \tag{2}$$

$$X^k_{i,j} = \sum_{l=j-k+1}^{j} D_{i,l}, \text{ if } j \geq k, \tag{3}$$

where $D_{i,l}$ is the $P-\mathrm{PET}$ difference in the first month of year i, in millimeters.

The probability density function of a three-parameter log-logistic distribution was employed to normalize the D series, in order to obtain the SPEI, as shown below:

$$f(x) = \frac{\beta}{\alpha}\left(\frac{x-\gamma}{\alpha}\right)^{\beta-1}\left[1+\left(\frac{x-\gamma}{\alpha}\right)^{\beta}\right]^{-2}, \tag{4}$$

where α, β, and γ denote the scale, shape, and origin, correspondingly, for D values in the range ($\gamma > D < \infty$).

Based on the log–logistic distribution, the probability distribution function of the D series is given by

$$F(x) = \left[1+\left(\frac{\alpha}{x-\gamma}\right)^{\beta}\right]^{-1}. \tag{5}$$

The computation of the SPEI is obtained through the standardized values of $F(x)$ as follows:

$$SPEI = W - \frac{C_0 + C_1 W + C_2 W}{1 + d_1 W + d_2 W^2 + d_3 W^3}, \tag{6}$$

where

$$W = \sqrt{-2\,\mathrm{In}(p)}, \tag{7}$$

$C_0 = 2.5155$, $C_1 = 0.8028$, $C_2 = 0.0203$, $d_1 = 1.4327$, $d_2 = 0.1892$, and $d_3 = 0.0013$. When $p \leq 0.5$, $W = \sqrt{-2\,\mathrm{In}(p)}$; when $p > 0.5$, $W = \sqrt{-2\,\mathrm{In}(1-p)}$.

As the SPEI is based on the SPI, negative and positive values indicate drought and wetness, respectively [98]. Based on this, we followed the classification of SPEI by Alley [14]. Here, the SPEI value indicates either extreme (SPEI ≤ -2.00), severe (-1.50 to -1.99), moderate (-1.00 to -1.49), or mild (-0.00 to -0.99) drought; likewise, it also can denote extreme (SPEI $\geq +2.00$), severe (+1.50 to +1.99), moderate (+1.00 to +1.49), or mild (+0.00 to +0.99) wetness. The frequency, duration, and intensity of drought and wetness events are characterized based on these SPEI values.

2.3.3. Computation of Drought/Wetness Characteristics

To compute the drought and wetness characteristics in the coastal Savannah agroecological zone of Ghana, thresholds of SPEI ≤ -1.00 and $\geq +1.00$ were used to capture drought and wetness events, respectively. We must emphasize that these events were also taken in terms of months. The recent studies of Ayugi et al. [47] on the evaluation of meteorological drought and flood scenarios over Kenya, East Africa, and that of Polong et al. [99] on the temporal and spatial evolution of the SPEI in the Tana River Basin, Kenya,

have employed similar thresholds. We adapted the definition of Ayugi et al. [47] to compute the frequency, duration, severity, and intensity of drought and wetness events.

Frequency indicates the number of occurrences of drought and wetness events in a given period, and is expressed as the ratio of the number of drought incidences in a month to the total number of months over the given period, calculated as follows:

$$F = \frac{n_k}{N_K} \times 100\%, \tag{8}$$

where F is the frequency of occurrence of a drought/wetness event/month, n_k indicates the number of drought (SPEI ≤ -1.00) and wetness (SPEI $\geq +1.00$) events, and N_k denotes the total number of months in the study period.

Duration (D) indicates the length of time (i.e., number of months) from the beginning to the end of drought or wetness events [6]. It is the sum of all drought and wetness event durations divided by the number of drought and wetness events [34], as expressed below, and is achieved by adding all the drought and wetness event periods and dividing by the number of droughts (in the case of drought events), and the same is done for wetness events.

$$D = \frac{\sum_{i=1}^{n} i}{K_S} \tag{9}$$

Here, D denotes the duration of drought/wetness events, n is the upper limit of the of drought/wetness duration events/months, i is the sum of drought/wetness duration events/months, and Ks is the number of drought/wetness events/months.

Severity (S) indicates the aggregate sum of the SPEI values, based on the duration amount, as expressed below:

$$\mathrm{S} = \sum_{i=1}^{\mathrm{D}} \mathrm{SPEI_i}, \tag{10}$$

where D is the duration, i is the month, and denotes the SPEIi value in month i.

The intensity (I) reveals the severity of a drought or wetness event over the duration of the drought or wetness event, and is computed by dividing severity in Equation (10) by the duration in Equation (9), as follows:

$$\mathrm{I} = \frac{\mathrm{S}}{\mathrm{D}}. \tag{11}$$

2.3.4. Trend Analysis

Mann–Kendall Test and Theil–Sen Slope Estimator

To analyze temporal trends in drought and wet events, the Mann–Kendall [100,101] (MK) test was conducted. The MK is a non-parametric test that compares the presence of a trend in a time-series to the null hypothesis that there is no trend [102]. The WMO strongly recommends the MK test when examining meteorological and hydrological variables [102,103], and it has been widely used in environmental research for temporal trend analysis [102,104]. The significance of the trends was tested in this study at the $\alpha = 0.05$ significance level. The Sen [105] slope estimator was employed to calculate the magnitude of the trend.

2.3.5. Spatial Interpolation

We employed the ordinary Kriging interpolation method to characterize drought and wetness events in the coastal Savannah agroecological zone of Ghana. The ordinary Kriging method is an effective surface interpolation technique that is based on spatially dependent variance and is normally expressed as a semivariogram [106,107]. The changes in 3 and 12

month SPEI values were examined by adapting the linear regression analysis with ordinary least squares and the slope trend analysis method [108], as follows:

$$S = \frac{l \times \sum_{p=1}^{l} a \times y_a - \sum_{p=1}^{l} a \sum_{p=1}^{l} y_a}{l \times \sum_{p=1}^{l} a^2 - \left(\sum_{p=1}^{l} a\right)^2}, \quad (12)$$

where S is the slope, which shows the trend of annual 3 and 12 month SPEI data; l is the length of the of the time-series; y_a reveals the mean value of SPEI at time i. Slopes greater than 0 (positive) and less than 0 (negative) indicate increasing and decreasing trends in drought and wetness events in the coastal Savannah agroecological zone, respectively.

3. Results

3.1. Changepoint Analysis

Table 1 shows the results of the changepoint analysis for temperature and rainfall for the study locations and the entire zone. Here, we employed the Pettitt, SNHT, and Buishand range homogeneity tests following the developed criteria (see Section 2.3.1). Table S1 provides a summary of the statistical results of the Pettitt, SNHT, and Buishand range homogeneity tests, and Figure S1 is a graphical depiction of the changepoints in the study region.

The overall results of the analysis in Table 1 reveal the homogeneous nature of both temperature and rainfall data. Notwithstanding, changepoints exist in most of the study locations. From Table 1, rainfall is more homogenous in the region than temperature. For instance, changepoints in temperature occurred in the years 1995, 1996, and 2002 in Accra and Tema, while a changepoint in rainfall occurred only in 2002. Again, in 1997, 2004, 2010, and 2012, changepoints were observed for temperature in Ada Foah, Anloga, and Keta, whereas rainfall was homogenous throughout the period. A similar case was observed in the locations of Cape Coast, Elmina, Moree, and Saltpond; the same is true for Apam, Bortianor, and Winneba (Table 1). From Table 1, the overall results for the entire zone reveal the homogeneous nature of both temperature and rainfall throughout the year for the period under analysis, except for September 1995 and November 2002 (for temperature and rainfall, respectively). Figure 2a,b show the changepoint occurrences in September 1995 for temperature and November 2002 for rainfall for the entire zone. Here, the results for the entire zone were obtained by averaging the results at individual locations.

Table 1. Changepoint analysis for temperature and rainfall. Note: * *HG* Homogeneous, * *CP* Change point, * *U* Uncertain.

Location	Month	Temperature		Rainfall	
		Nature of Series	Year of Change	Nature of Series	Year of Change
Accra, Tema	Jan	HG	–	HG	–
	Feb	HG	–	HG	–
	Mar	CP	1996	HG	–
	Apr	HG	–	HG	–
	May	HG	–	HG	–
	Jun	HG	–	HG	–
	Jul	HG	–	HG	–
	Aug	HG	–	HG	–
	Sep	CP	2002	HG	–
	Oct	CP	1995	U	–
	Nov	HG	–	CP	2002
	Dec	HG	–	HG	–
	Annual	HG	–	HG	–

Table 1. *Cont.*

Location	Month	Temperature		Rainfall	
		Nature of Series	Year of Change	Nature of Series	Year of Change
Ada Foah, Anloga, Keta	Jan	HG	–	HG	–
	Feb	HG	–	HG	–
	Mar	HG	–	HG	–
	Apr	HG	–	HG	–
	May	HG	–	HG	–
	Jun	CP	2010	HG	–
	Jul	CP	1997	HG	–
	Aug	CP	2012	HG	–
	Sep	CP	2004	HG	–
	Oct	HG	–	HG	–
	Nov	HG	–	U	–
	Dec	HG	–	HG	–
	Annual	HG		HG	–
Cape Coast, Elmina, Moree, Saltpond	Jan	HG	–	HG	–
	Feb	HG	–	CP	2002
	Mar	CP	1996	HG	–
	Apr	HG	–	HG	–
	May	CP	1997	HG	–
	Jun	HG	–	HG	–
	Jul	HG	–	HG	–
	Aug	HG	–	HG	–
	Sep	CP	2002	HG	–
	Oct	CP	1996	HG	–
	Nov	CP	1996	U	–
	Dec	HG	–	HG	–
	Annual	CP	1997	HG	–
Apam, Bortianor, Winneba	Jan	HG	–	HG	–
	Feb	HG	–	HG	–
	Mar	HG	–	HG	–
	Apr	HG	–	HG	–
	May	HG	–	HG	–
	Jun	HG	–	HG	–
	Jul	HG	–	HG	–
	Aug	HG	–	HG	–
	Sep	CP	2002	HG	–
	Oct	CP	1995	U	–
	Nov	HG	–	CP	1999
	Dec	HG	–	HG	–
	Annual	HG	–	HG	–
Prampram	Jan	HG	–	HG	–
	Feb	HG	–	HG	–
	Mar	HG	–	HG	–
	Apr	HG	–	HG	–
	May	HG	–	HG	–
	Jun	HG	–	HG	–
	Jul	HG	–	HG	–
	Aug	HG	–	HG	–
	Sep	CP	1995	HG	–
	Oct	HG	–	HG	–
	Nov	HG	–	CP	2002
	Dec	HG	–	HG	–
	Annual	HG	–	HG	–

Table 1. *Cont.*

Location	Month	Temperature		Rainfall	
		Nature of Series	Year of Change	Nature of Series	Year of Change
Denu	Jan	HG	–	HG	–
	Feb	HG	–	HG	–
	Mar	CP	1997	HG	–
	Apr	HG	–	HG	–
	May	HG	–	HG	–
	Jun	HG	–	HG	–
	Jul	CP	2005	HG	–
	Aug	HG	–	HG	–
	Sep	CP	2002	HG	–
	Oct	U	–	HG	–
	Nov	CP	1994	U	–
	Dec	HG	–	HG	–
	Annual	HG	1997	HG	–
Entire zone	Jan	HG	–	HG	–
	Feb	HG	–	HG	–
	Mar	HG	–	HG	–
	Apr	HG	–	HG	–
	May	HG	–	HG	–
	Jun	HG	–	HG	–
	Jul	HG	–	HG	–
	Aug	HG	–	HG	–
	Sep	CP	1995	HG	–
	Oct	HG	–	HG	–
	Nov	HG	–	CP	2002
	Dec	HG	–	HG	–
	Annual	HG	–	HG	–

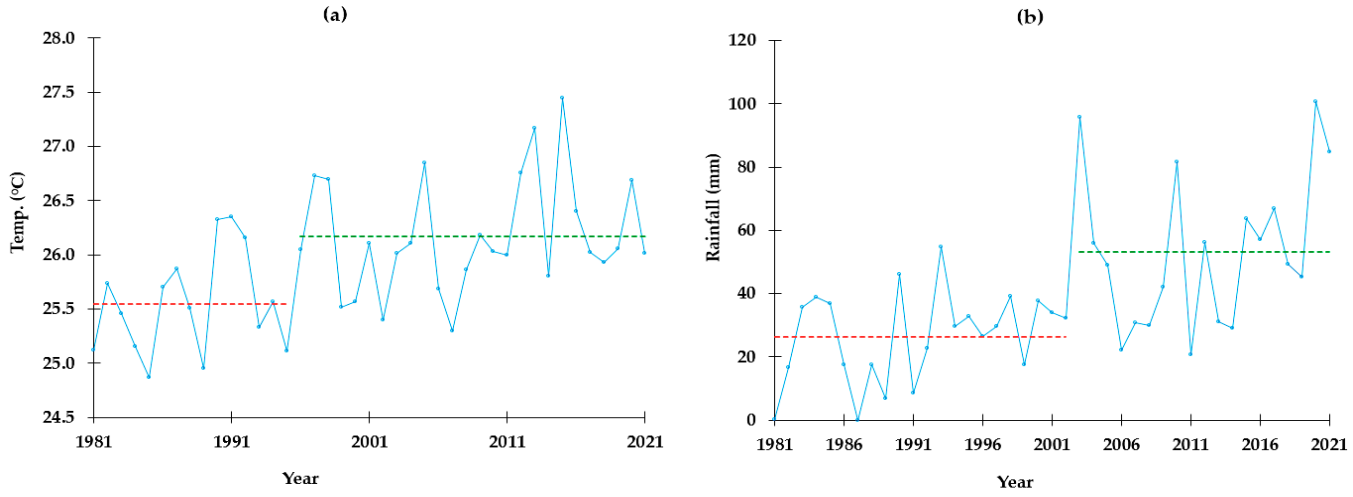

Figure 2. Changepoints in September temperature (**a**) and November rainfall (**b**) for the coastal Savannah agroecological zone of Ghana.

3.2. Monthly Variations in Drought and Wetness Events

Figure 3a–d show the mean monthly variations in SPEI-3 and SPE-12 drought and wetness events over the coastal Savannah agroecological zone of Ghana from 1981 to 2021. Here, we analyzed the monthly variations in moderate, severe, and extreme drought events (Figure 3a,b) and wetness events (Figure 3c,d) for SPEI-3 and SPEI-12 based on the thresholds of ≤ -1.00 (drought) and $\geq +1.00$ (wetness). Table 2 shows the results of the Mann–Kendal test and Sen's slope estimate for the monthly variations in moderate-

to-extreme drought and wetness events under the SPEI-3 and SPEI-12 timescales. From Figure 3a, it can be observed that extreme drought events were more common in the dry season (late November–March) than in the wet season (April–July) under the SPEI-3 timescale. Notwithstanding, moderate-to-severe drought events occurred throughout the season, except for June and July, when no moderate drought events occurred. The SPEI-12 timescale (Figure 3b) revealed that extreme drought events are typical throughout the season, except for the months of June and July, while moderate-to-severe drought events occurred across the season.

From Figure 3c,d, it can be seen that the zone experienced moderate-to-extreme wetness events throughout the months under the period of analysis. Notwithstanding, moderate-to-extreme wetness events were stronger in the wet season (April–July) than in the minor season (September–early November) and the dry season (late November–March), under both the SPEI-3 and SPEI-12 timescales.

The results of the Mann–Kendall test revealed a positive significant trend (alpha: 0.05, *p*-value: 0.042), but a weak magnitude of change (Sen's slope estimate: 0.000) only in moderate drought throughout the months in the zone under the SPEI-12 (Table 2). Among the seasons, a significant positive trend (alpha: 0.05, *p*-value: 0.037), but a weak magnitude of change (Sen's slope estimate: 0.010), only existed in the dry season for severe wetness under the SPEI-3, with the others being non-significant (Table 2).

The incidences of drought and wetness events in the coastal savannah agroecological zone tended to follow the seasonal patterns in temperature and rainfall in the zone. While extreme drought event occurrences were greater in the month of January (values of −2.7 and −2.3, for SPEI-3 and SPEI-12, respectively), the corresponding extreme wetness event incidences were greater in June (2.6 and 2.3 for SPEI-3 and SPEI-12, correspondingly) during the wet season and in October (2.3 under both SPEI-3 and SPEI-12) for the minor season.

Table 2. Mann–Kendall trend test and Sen's slope estimate for seasonal drought and wetness events from 1981–2021.

Index	Drought/Wet Events	MK Stat (S)	Var (S)	Kendall's Tau	*p*-Value	Sen's Slope
			All months			
SPEI-3 (SPEI-12)	Moderate drought	13 (19)	186.333 (87.667)	0.229 (0.510)	0.341 (0.042 *)	0.000 (0.000)
	Severe drought	7 (21)	146.333 (198.333)	0.144 (0.349)	0.563 (0.136)	0.000 (0.017)
	Extreme drought	7 (4)	15.667 (114.000)	0.738 (0.099)	0.077 (0.708)	0.065 (0.000)
	Moderate wet	12 (18)	164.667 (164.667)	0.228 (0.342)	0.350 (0.161)	0.000 (0.000)
	Severe wet	24 (13)	193.333 (139.667)	0.410 (0.281)	0.084 (0.271)	0.013 (0.000)
	Extreme wet	−9 (−4)	151.667 (145.333)	−0.181 (−0.083)	0.465 (0.740)	0.000 (0.000)
			Wet season			
SPEI-3 (SPEI-12)	Moderate drought	5 (?)	7.667 (?)	0.913 (?)	0.071 (?)	0.083 (?)
	Severe drought	5 (5)	7.667 (7.667)	0.913 (0.913)	0.071 (0.071)	0.100 (0.100)
	Extreme drought	*NA* (?)	*NA* (?)	*NA* (?)	*NA* (?)	*NA* (?)
	Moderate wet	4 (1)	8.667 (5.000)	0.667 (0.236)	0.174 (0.655)	0.083 (0.000)
	Severe wet	3 (0)	7.667 (2.667)	0.548 (0)	0.279 (1.000)	0.067 (0.000)
	Extreme wet	3 (3)	7.667 (7.667)	0.548 (0.548)	0.279 (0.279)	0.042 (0.067)
			Minor season			
	Moderate drought	2 (?)	2.667 (?)	0.816 (?)	0.221 (?)	0.050 (?)
	Severe drought	*NA* (−2)	*NA* (2.667)	*NA* (−0.816)	*NA* (0.221)	*NA* (−0.050)
	Extreme drought	1 (0)	1.000 (2.667)	1 (0)	0.317 (1.000)	0.050 (0.000)
SPEI-3 (SPEI-12)	Moderate wet	0 (2)	2.667 (2.667)	0 (0.816)	1.000 (0.221)	0.000 (0.050)
	Severe wet	1 (?)	3.667 (?)	0.333 (?)	0.602 (?)	0.050 (?)
	Extreme wet	0 (0)	2.667 (2.667)	0 (0)	1.000 (1.000)	0.000 (0.000)
			Dry season			
	Moderate drought	1 (5)	13.000 (13.000)	0.120 (0.598)	0.782 (0.166)	0.000 (0.012)
	Severe drought	0 (7)	8.000 (13.000)	0 (0.837)	1.000 (0.052)	0.000 (0.021)
SPEI-3 (SPEI-12)	Extreme drought	4 (4)	8.667 (14.667)	0.667 (0.447)	0.174 (0.296)	0.066 (0.011)
	Moderate wet	4 (4)	8.000 (14.667)	0.632 (0.447)	0.157 (0.296)	0.000 (0.010)
	Severe wet	8 (5)	14.667 (13.000)	0.894 (0.598)	0.037 * (0.166)	0.012 (0.010)
	Extreme wet	−1 (−1)	5.000 (5.000)	−0.236 (−0.236)	0.655 (0.655)	0.000 (0.000)

Note: * Significant at 0.05, Reject H_o if *p*-value is < 0.05 or accept H_o if *p*-value is > 0.05. *NA* Not applicable, or the event did not appear in a specific index or season. ? The event could not be computed as some sequences were constant.

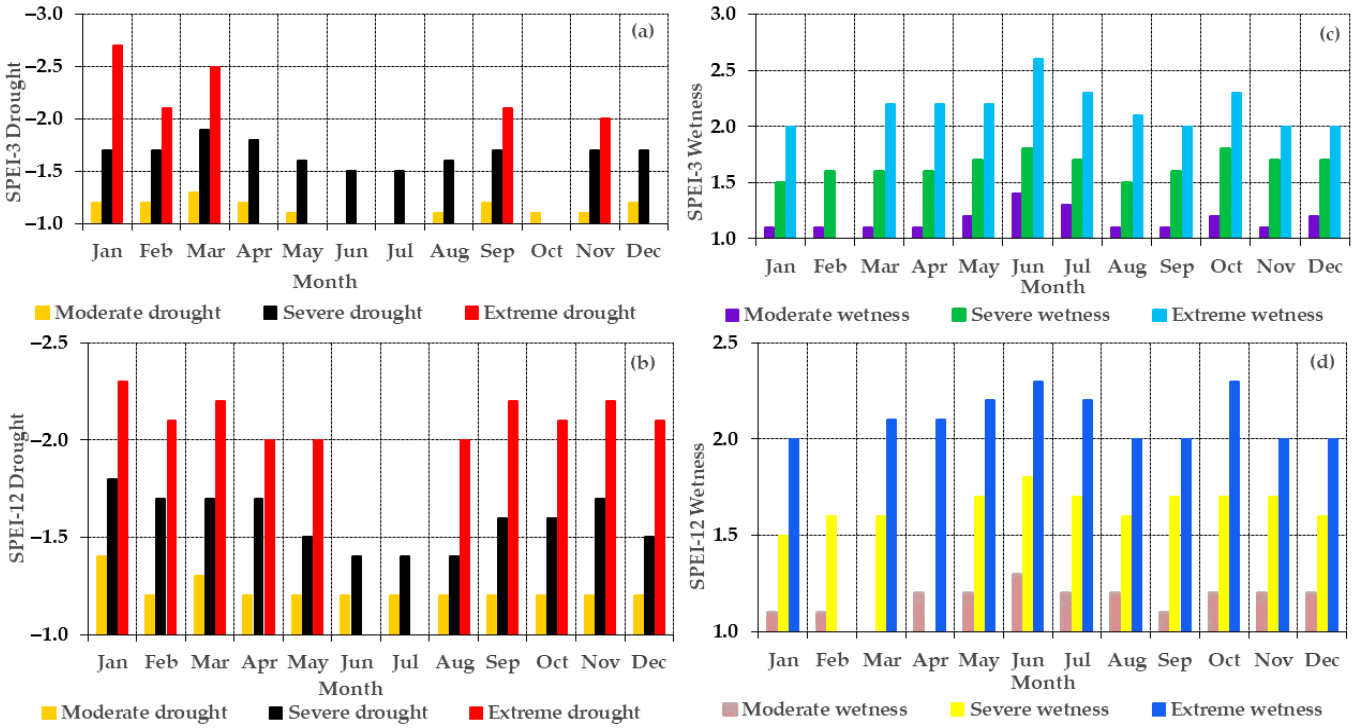

Figure 3. Temporal evolution of the mean monthly SPEI-3 and SPEI-12 for moderate, severe, and extreme drought (**a**,**b**) and wetness (**c**,**d**) from 1981–2021 over the coastal Savannah agroecological zone in Ghana.

Temporal Evolution and Trends in Drought and Wetness Events

Figure 4a–e show the temporal evolution of drought and wetness events over the coastal Savannah agroecological zone of Ghana from 1981 to 2021. We analyzed the temporal developments in moderate-to-extreme drought (Figure 4a,b) and wetness (Figure 4c,d), as well as all drought and wetness events (Figure 4e) for SPEI-3 and SPEI-12, following the thresholds of ≤ -1.00 (drought) and $\geq +1.00$ (wetness). All drought and wetness events in the zone were calculated using the averages of moderate-to-extreme drought and wetness events. It should be noted that the normal drought and wetness categories were not considered in this study, based on the established thresholds. It is apparent, from Figure 4a,b, that the study region has suffered moderate-to-extreme drought events, notwithstanding the wet event incidences (Figure 4c,d). For instance, in Figure 4a, the SPEI-3 detected moderate-to-extreme drought events in the 1980s and 1990s and moderate-to-severe in the 2000s, except for the year 2009, when an extreme event happened. Under the SPEI-3 timescale, extreme drought events occurred in the years 1983 (value: −2.7), 1990 (−2.0), 1992 (−2.3), 1996 (−2.0), 1998 (−2.3), and 2009 (−2.0). Similar drought events were also detected under the SPEI-12 timescale (Figure 4b). However, the moderate-to-extreme and moderate-to-severe drought event incidences were higher for the SPEI-3 data. For example, extreme drought events under SPEI-12 appeared only in the 1980s and 1990s, and not in the 2000s, as was the case with SPEI-3. Here, the extreme drought years occurred in 1983 (value: −2.3), 1984, 1993 (−2.3), and 1998 and 1999 (−2.0).

The study region also observed moderate-to-extreme wetness events on both the SPEI-3 and SPEI-12 timescales (Figure 4c,d). In Figure 4c, the SPEI-3 recorded moderate-to-extreme wetness events in the 1980s and 1990s and moderate-to-severe ones in the 2000s, excluding the year 2021, when an extreme wetness event ensued. Extreme wetness events occurred in 1987 (value: 2.5), 1991 (2.0), and in 1997 and 2021 (2.2). The SPEI-12 timescale also recorded moderate-to-severe wetness events in the 1980s and 1990s and moderate-to-extreme wetness events in the 2000s, with the years 2021 (value: 2.2) and 2020 (2.0) recording extreme wetness events.

From Figure 4e, it is evident that drought and wetness events are common in the zone. The years 1983 and 1999 recorded the greatest drought incidences, with the highest values (−2.0) under the SPEI-12 timescale, while the lowest (−1.0) occurred in 1981, 1994, 2012, and 2017 under the SPEI-3 timescale (Figure 4e). The year 1987 recorded the highest value (2.5) of a wetness event under the SPEI-3 timescale, followed by 2021 (2.0) for the SPEI-12 timescale, and the lowest (1.0) occurring in 1982 and 1992 (under SPEI-12) and 1995 and 1999 (under SPEI-3). Under the SPEI-12 timescale, a low value (1.0) followed in 2016. Figure S2 depicts the results of the temporal developments in drought and wetness events for the individual study locations.

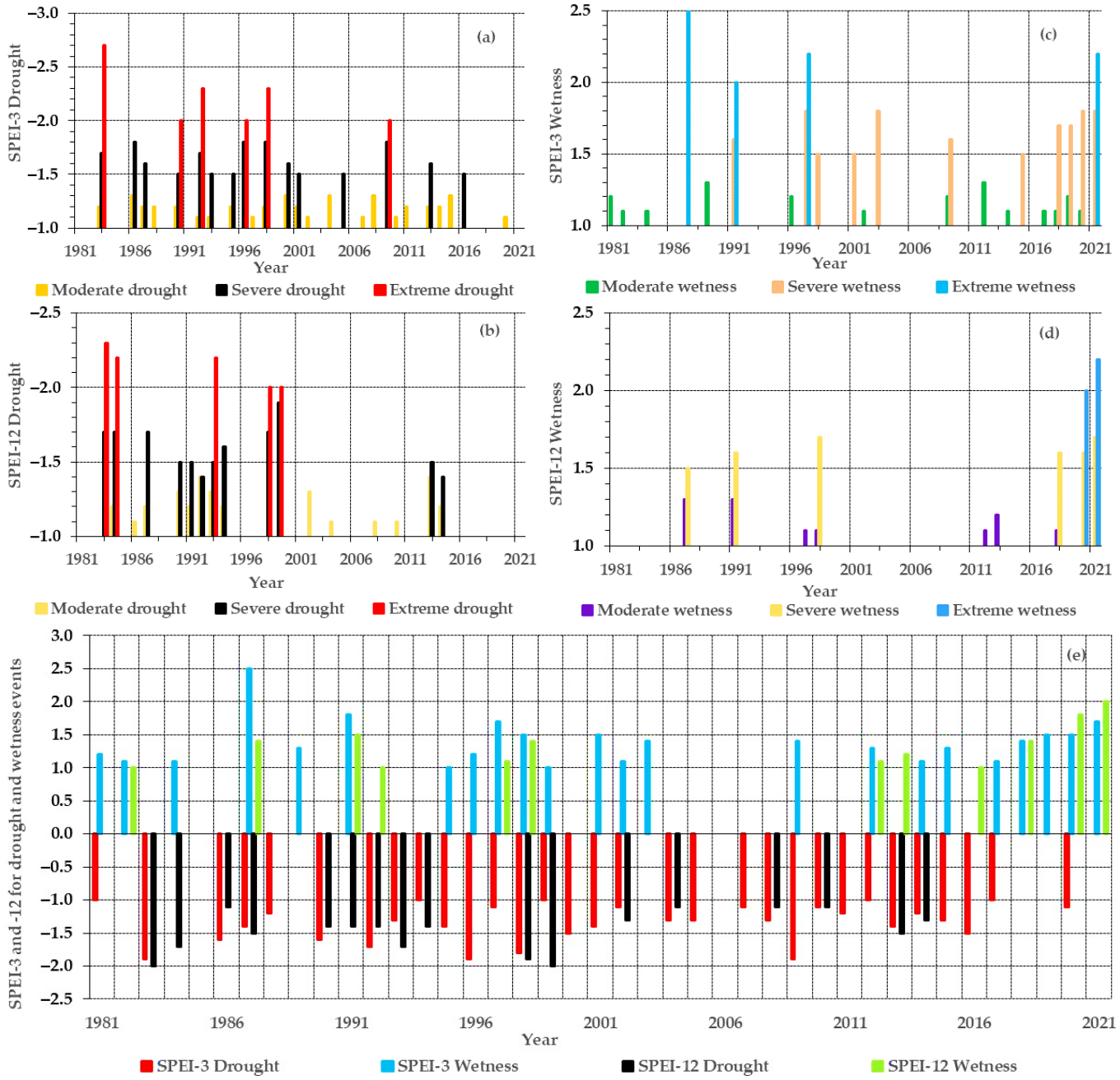

Figure 4. Temporal evolution of the mean annual SPEI-3 and SPEI-12 for moderate-to-extreme drought (**a**,**b**), wetness (**c**,**d**), and all drought and wet events (**e**) from 1981–2021 over the coastal Savannah agroecological zone in Ghana.

The results of the Mann–Kendall test (Table 3) showed a significant positive trend (alpha: 0.05, *p*-value: 0.037) in the extreme drought events in the zone. However, the magnitude of change was weak (Sen's slope estimate: 0.017). No significant trends were observed in the other drought groups, and the same was true for all drought and wetness events (Table 3).

Table 3. Mann–Kendall trend test and Sen's slope estimate for annual drought and wetness events from 1981–2021.

Index	Drought/Wetness Event	MK Stat (S)	Var (S)	Kendall's Tau	*p*-Value	Sen's Slope
SPEI-3 (SPEI-12)	Moderate drought	13 (1)	2347.667 (303.667)	0.039 (0.012)	0.788 (0.954)	0.000 (0.000)
	Severe drought	16 (13)	366.667 (194.333)	0.175 (0.220)	0.403 (0.351)	0.000 (0.002)
	Extreme drought	5 (8)	23.667 (14.667)	0.389 (0.894)	0.304 (0.037 *)	0.018 (0.017)
	Moderate wetness	−16 (−3)	734.667 (111.667)	−0.108 (−0.076)	0.555 (0.776)	0.000 (0.000)
	Severe wetness	16 (7)	150.667 (23.667)	0.325 (0.545)	0.192 (0.150)	0.007 (0.003)
	Extreme wetness	−−1 (1)	7.667 (1.000)	−0.183 (1)	0.718 (0.317)	−0.004 (0.200)
SPEI-3(SPEI-12)	All drought	91 (38)	33,993.667 (568.000)	0.206 (0.297)	0.118 (0.111)	0.008 (0.011)
	All wetness	32 (23)	1398.000 (204.333)	0.133 (0.369)	0.392 (0.108)	0.005 (0.012)

Note: * Significant at 0.05, Reject H_o if *p*-value is < 0.05 or accept H_o if *p*-value is > 0.05.

3.3. Spatial Evolution of SPEI

Figure 5a–h shows the spatial evolution of the occurrences of extreme and severe drought and wetness events in SPEI-3 and SPEI-12 over the coastal Savannah agroecological zone. At this point, an analysis was conducted to identify the distribution of extreme and severe drought and wetness events across the study region, following the earlier analysis. Here, the analysis was carried out following the region classification (see Figure 1). Notably, extreme dry events have SPEI values of ≤ -2.00 and represent the worst drought events in the region, whereas severe dry events have SPEI values ranging from -1.50 to -1.99, indicating intense drought conditions. In Figure 5a,b, the SPEI-3 recorded a high occurrence (2.03) of extreme drought events in most parts of Central and Greater Accra and a low occurrence (0.61) in Volta. According to the SPEI-12, there were both high (3.64) and low (0.20) occurrences of extreme drought in the Central and Greater Accra, with a low value in Volta. A dissimilar pattern was observed regarding severe drought events over the study region. Here, high incidences of severe drought events (Figure 5c,d) appeared in the Volta under the SPEI-3 and SPEI-12 (7.52 and 9.15, respectively). Both SPEI-3 and SPEI-12 were able to detect severe drought events in some parts of Central and Greater Accra.

Regional variations were also observed regarding the extreme and severe wetness events (Figure 5e–h). In Figure 5e, the SPEI-3 identified the maximum (2.64) incidence of extreme wetness events in the Central and some areas of Greater Accra and Volta, while the minimum (1.22) occurred for Greater Accra and Volta. Under the SPEI-12 (Figure 5f), a greater (3.46) occurrence of extreme wetness was observed in Central, with moderate-to-extreme events in Greater Accra, and the lowest occurrence (0.20) in Volta. In Figure 5g,h, high occurrences of severe wetness events occurred in Volta and some parts of Greater Accra (8.33 and 6.91, respectively), and low occurrences (2.85 and 3.05) were observed in Central.

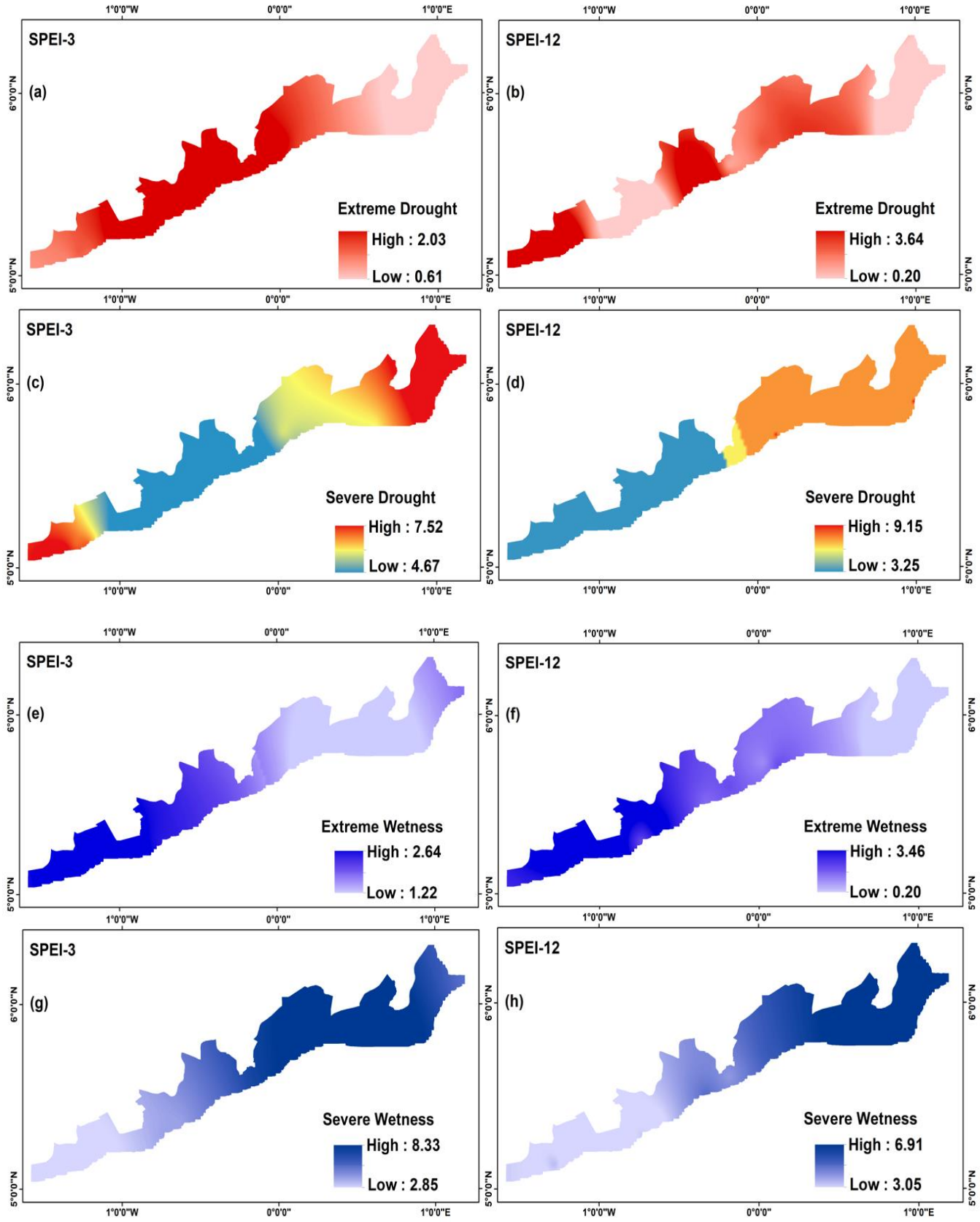

Figure 5. Spatial distribution of the average values for SPEI-3 and SPEI-12 for extreme drought (**a**,**b**), severe drought (**c**,**d**), extreme wetness (**e**,**f**), and severe wetness (**g**,**h**) events in the coastal Savannah agroecological zone of Ghana from 1981 to 2021.

3.4. Spatial Distribution of Drought and Wetness Characteristics

Considering the definitions provided in Section 2.3.3, we characterized drought and wetness events in the coastal Savannah agroecological zone of Ghana based on their frequency, duration, and intensity (Figure 6a–l). In terms of percentage, high values (20.9) occurred in the areas of Volta and some parts of Central, while a low one (17.3) appeared in Greater Accra and Central under the SPEI-3 (Figure 6a). A similar pattern was observed with the SPEI-12, where the highest frequency (21.3) was seen in Volta and some parts of Central and Greater Accra, with the lowest (15.0) also occurring in the latter two regions (Figure 6b). In the corresponding wetness frequency (Figure 6g,h), the maximum (19.9) and minimum (16.9) were distributed across the regions for the SPEI-3 (Figure 6g). As can be seen from Figure 6h, while the greatest value (19.9) occurred across the regions, it was superior in Volta, compared to the other two. The lowest (13.8) occurred in most parts of Central.

In Figure 6c,d, the drought duration varied across the regions. Drought duration was much longer in Central and Greater Accra than in Volta under both SPEI-3 (a high of 1.44) and SPEI-12 (1.57), as shown in Figure 6c,d. For SPEI-3 (Figure 6i), a high (1.47) and a low (1.39) duration of wetness events occurred across the zone. However, in SPEI-12, the greatest (1.54) wetness duration appeared for the Central portion, with the lowest (1.37) occurring for the other two regions (Figure 6j). The intensity of the drought (Figure 6e,f) and wetness (Figure 6k,l) followed a similar pattern to that of the duration. For example, in Figure 6e,f, the intensity of the drought cuts across the regions with the highest intensities of 1.50 and 1.64 under the SPEI-3 and SPEI-12 timescales, respectively. The intensity of wetness events identified by SPEI-3 (Figure 6k) was also distributed across the regions, while that of SPEI-12 (Figure 6l) was more intense in the Central region than the other two. A clear local variation was also observed in the drought and wetness frequencies, durations, and intensities across the zone.

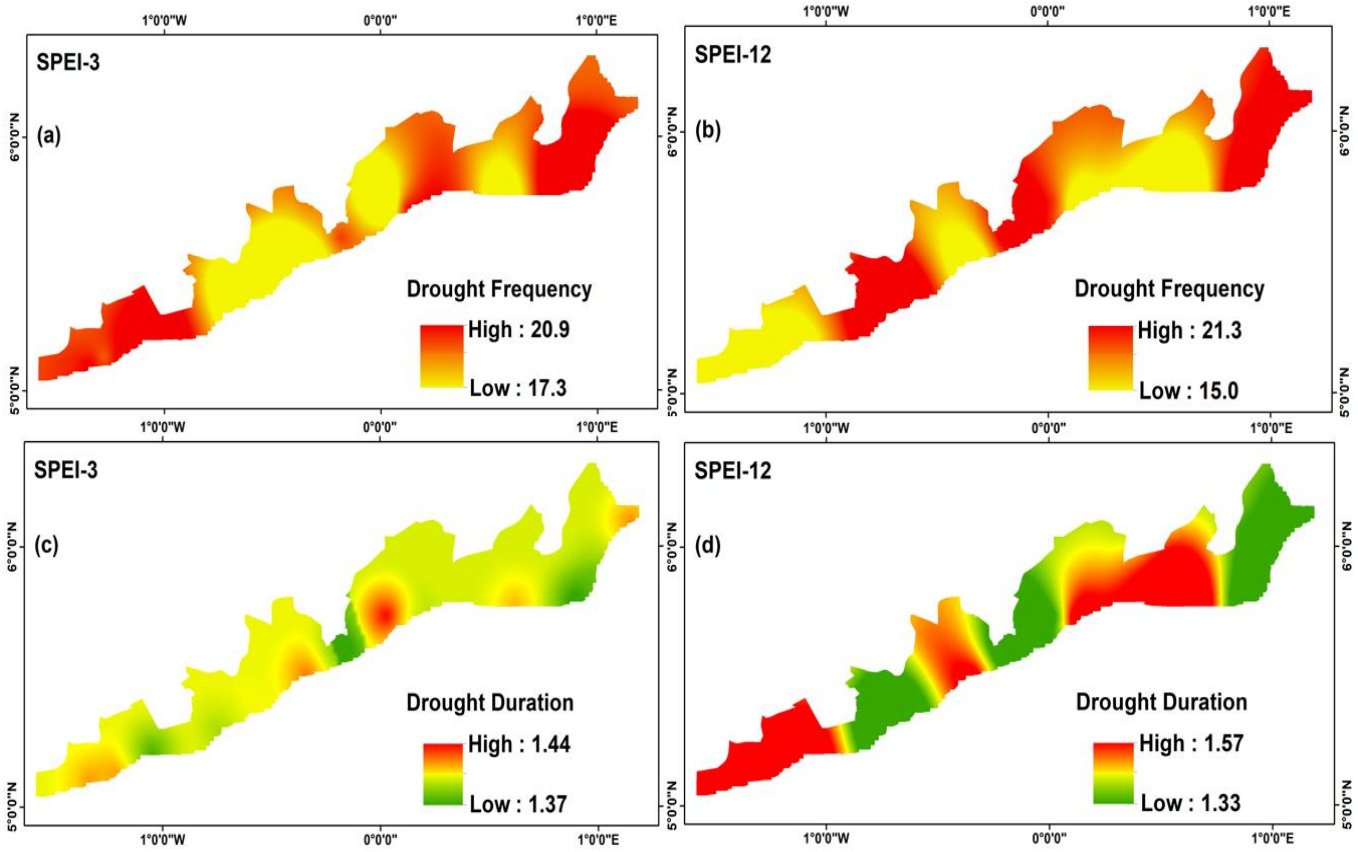

Figure 6. *Cont.*

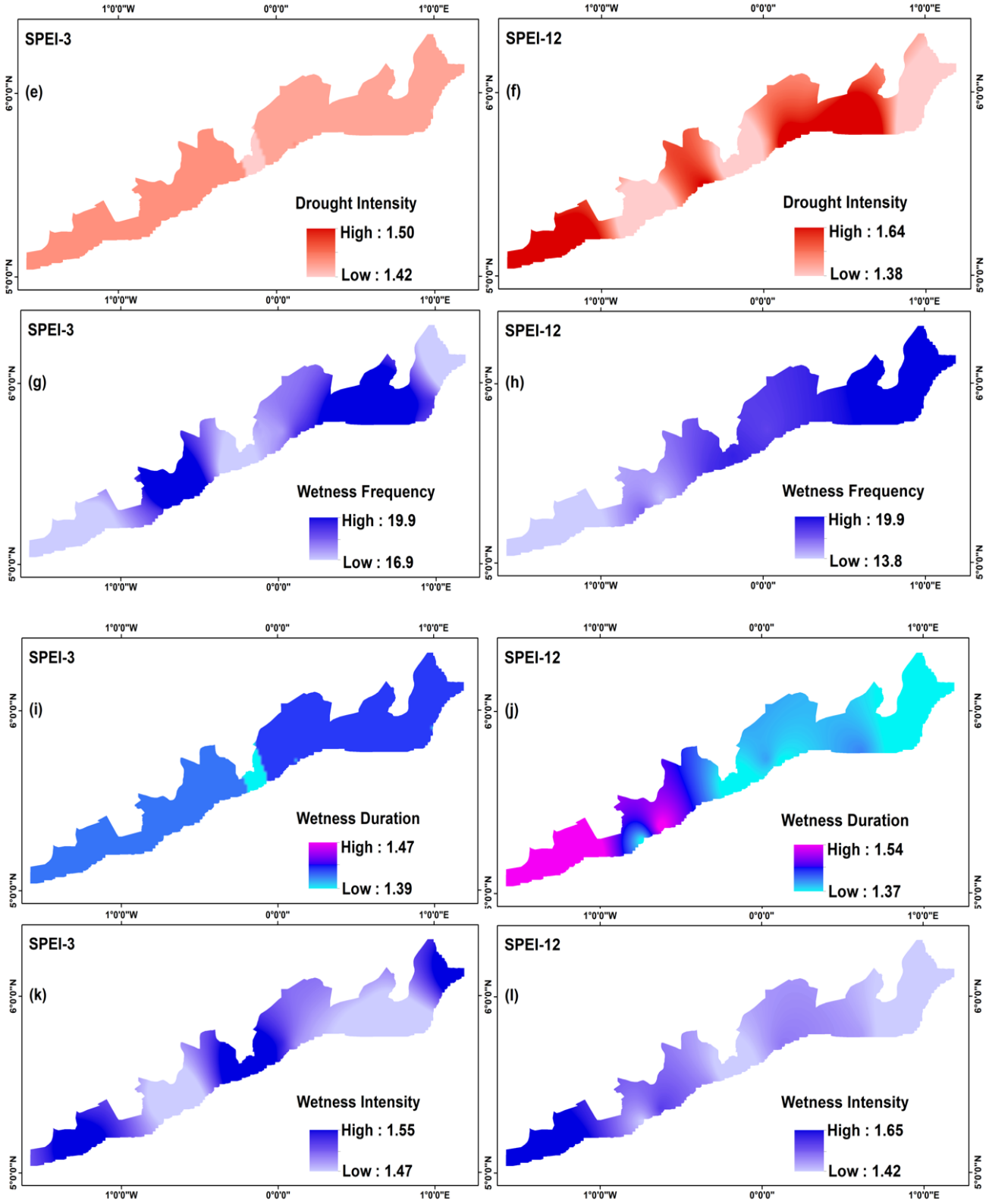

Figure 6. Spatial distribution of drought and wetness characteristics at SPEI-3 and SPEI-12 timescales in the coastal Savannah agroecological of Ghana from 1981–2021: Drought frequency (**a**,**b**) SPEI-3 and SPEI-12; drought duration (**c**,**d**) SPEI-3 and SPEI-12; drought intensity (**e**,**f**) SPEI-3 and SPEI-12; wetness frequency (**g**,**h**) SPEI-3 and SPEI-12; wetness duration (**i**,**j**) SPEI-3 and SPEI-12; wetness intensity (**k**,**l**) SPEI-3 and SPEI-12.

3.5. Spatial Distribution of Drought and Wetness Trends

Figure 7a–d show the spatial distribution of drought and wetness trends in the coastal Savannah agroecological zone of Ghana from 1981 to 2021 for SPEI-3 and SPEI-12 timescales using linear regression analysis with ordinary least squares. For SPEI-3 (Figure 7a), the drought trends were greater (0.157) in the Central and Volta areas and less (−0.000) for Greater Accra. Under SPEI-12, high (0.043) trends appeared for the Central region and were low (−0.027) for the other two regions (Figure 7b). In Figure 7c, maximum (0.040) wetness trends occurred in the Central and Greater Accra areas, while a minimum (0.002) was observed in the Volta under SPEI-3. For SPEI-12 (Figure 7d), higher (0.056) wet trends were observed in the Greater Accra area and some parts of the Central region.

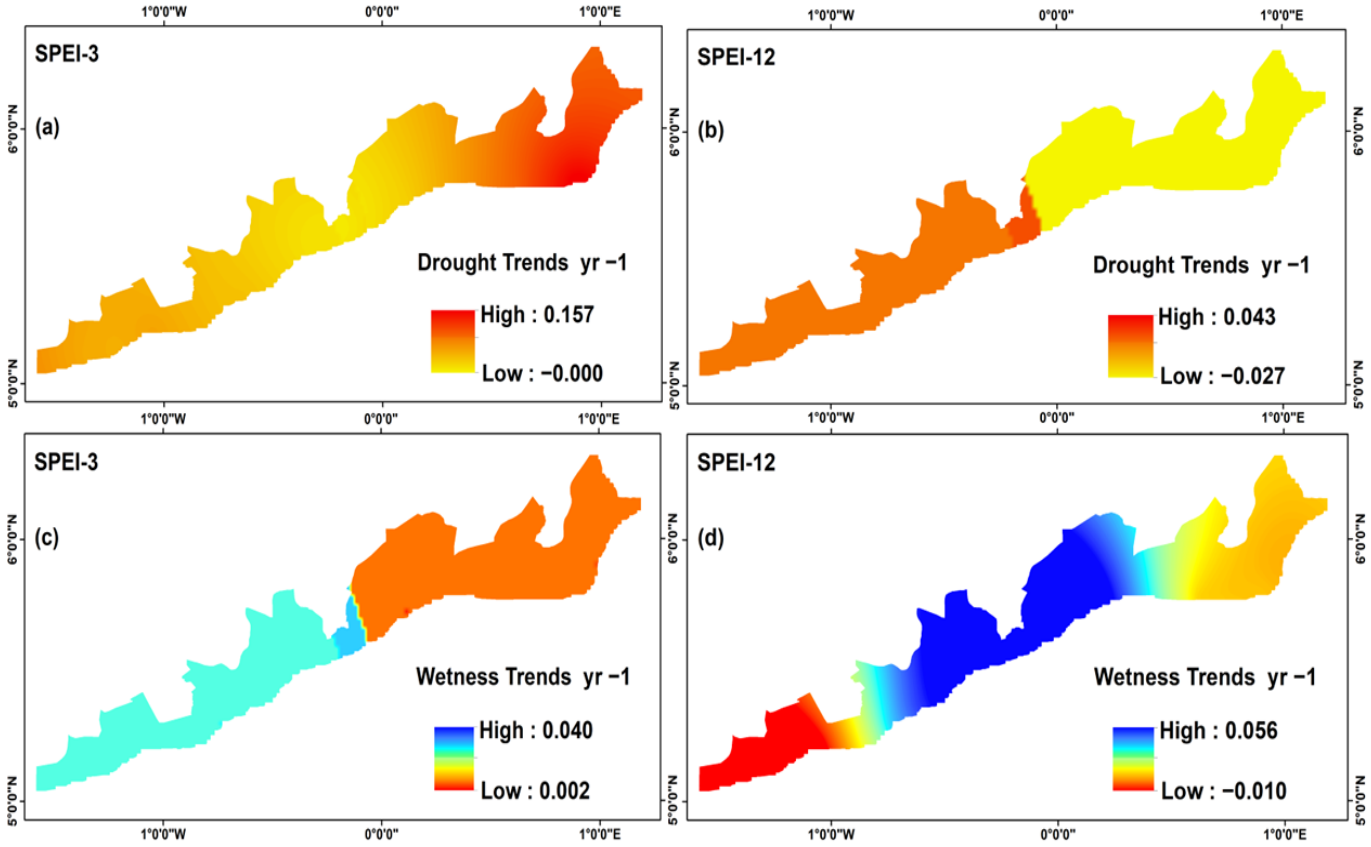

Figure 7. Spatial distribution of drought/wetness trends in the coastal Savannah agroecological zone of Ghana: Drought trends under (**a**) SPEI-3 and (**b**) SPEI-12 timescales; wetness trends under (**c**) SPEI-3 and (**d**) SPEI-12 timescales.

Drought in the zone increased from Central to Volta during the period of analysis. While the corresponding wetness followed a similar pattern, the increase was greater in the Greater Accra area. Here, it is important not to disregard the local variations in drought and wet trends across the regions.

4. Discussion

The occurrence of extreme events, such as droughts and wetness, has become common in many regions of the world due to anthropogenic-induced global warming [41]. Of course, large-scale natural variability, such as the El Niño Southern Oscillation (ENSO), also has an impact on the occurrence of extreme climatic events [109,110]. However, the evidence of harmful anthropogenic activities and related greenhouse gas emissions is apparent, as has been reiterated by the IPCC [41]. Variability has become a common characteristic of the climates of many countries, especially in the parameters of temperature and precipitation.

Variations in these climatic parameters are possibly the cause of drought and wet events in the coastal Savannah agroecological zone of Ghana, taking into consideration the role of rainfall and temperature on evapotranspiration. As has been highlighted by Thiaw and Kumar [66], extreme events and natural disasters are inherent elements of the West African climate, and Ghana's in particular.

The results of the changepoint analysis revealed the homogeneous nature of rainfall and temperature in the study region. Nonetheless, there were significant temperature changes between the mid-1990s to 2012. The changepoints in the climate variables could be attributed to the increased industrial and commercial activities in the zone, especially in the capital city (Accra) and Tema. The above finding is consistent with earlier studies conducted elsewhere, such as in southeast Australia [94], Raipur (the capital city of Chhattisgarh state, India) [95], and in Umbria, Italy [111].

Despite the corresponding wetness incidences, our findings clearly established the frequency and intensity of drought events. These findings support previous studies conducted in different regions of the world [99,112–115]. For instance, Wang et al. [112] have reported an increased frequency and intensity of drought events in the Yellow River Basin in China. An et al. [113] have reported a significant increase in the frequency and intensity of droughts in Inner Mongolia. Similarly, Ge et al. [114] have revealed aggravated drought frequency, intensity, and duration in the northern and eastern Indian plains. The study region's combined drought and wetness events may endanger the livelihood opportunities of many people. For instance, while the extreme drought events in the 1980s and 1983 in particular were so extreme, the flood occurrences in 2013 in the study region (and Accra, to be precise) negatively affected the livelihoods of the people and led to related mortalities [116]. Undoubtedly, the immense consequences for agriculture cannot be ignored, especially considering the rainfed nature of agriculture in the study region. There is significant evidence of the impacts of drought on agriculture in the scientific literature. Research studies such as [117–123] have reported the dire impacts of drought on agriculture. Smallholder farmers in the zone are, thus, vulnerable to these extreme events. Despite the fact that wetness events in the study region have recently increased, there is evidence of significant losses to the livelihoods of smallholder farmers in the region caused by floods [124]. The ongoing drought and wetness events will have implications for food security in the study region, and Ghana as a whole. This is obvious, especially given the frequency of moderate-to-extreme and moderate-to-severe drought/wetness events in the short-term timescale (SPEI-3; see Figure 4), indicating that drought/wetness events have a greater impact on agriculture during the growing season than on hydrological and water resources in the study region [19,125].

The monthly variations revealed that drought and wetness event incidences follow the seasonal pattern in temperature and rainfall in the zone. While moderate-to-severe drought and wetness events were common throughout the season, extreme drought event occurrences were greater in the dry season, especially in January, while the corresponding extreme wetness event values were higher in June and October. The results emphasized short- and long-term variations in drought and wetness events across the study region. In both the short- and long-term timescales, the incidence of extreme drought or wetness events was higher in the Central and Greater Accra areas than in Volta (see Figure 5), despite local variability across the regions. This was similar, in terms of the duration and intensity of drought or wet events (see Figure 6). Drought or wetness events increased from the Central region to the Volta. The above finding is in line with the earlier study by Santos et al. [126] conducted in Portugal, which reported the increased occurrence of more frequent cycles of drought and wet events in the south of Portugal, compared to the north. The finding also supports the study of Zhao et al. [127], who observed increased wetter and fewer drought conditions in the western upstream part of the Yangtze River Basin, China. The variations in drought or wetness events across the study region are possibly the result of the atmosphere–ocean–land connections, or due to the differences in topography and landscape dynamics. For instance, the changes in drought and wetness events in

the study region (and Ghana in general) have been linked to the seasonal movements in the Intertropical Discontinuity (ITD) and the West African Monsoon winds [78]. The ITD develops when the dry northeast trade winds (originating from the Sahara Desert) meet the moist southwest (originating from the South Atlantic Ocean) trade winds. The movement of the ITD is responsible for the seasonal rainfall patterns in Ghana. The seasonal movement of the ITD from the north to the south (and vice versa) results in more drought and wetness events, respectively. Furthermore, ocean–atmosphere dynamics, evidenced by abnormal sea surface temperatures and related large-scale teleconnection factors, such as the ENSO and the North Atlantic Oscillation (NAO), are related to the occurrences of extreme events in West Africa, and Ghana in particular [78]. Other climate change attribution studies have also stressed the increased incidence of frequent and intense droughts and wetness events. Dai [3] reviewed drought events under global warming and established that drought periods that lasted for years to decades have occurred many times in West Africa, North America, and East Asia. Similarly, Chiang et al. [128] have reported increased drought frequency, intensity, and duration in larger parts of the Americas, Africa, and Asia due to anthropogenic forcing. In addition, Brito et al. [129] have revealed the frequent nature of drought conditions in the semi-arid Northeast region of Brazil. Christidis and Stott [130] further stated that drought conditions are more prevalent in the south of Europe than in the north of Europe, while the opposite is true for wet conditions, due to the influence of anthropogenic climate change. Furthermore, due to the significant temperature rise, increased drought events have occurred in the Mediterranean region, while precipitation has remained stable or decreased [131–133]. Both drought and wetness events are projected to increase as a result of human-induced global warming [134,135].

Although we selected the 3 and 12 month timescales, several research studies, such as [34,136,137], have reported the feasibility of considering other timescales. Drought and wetness analyses can be performed on a variety of timescales, depending on the need.

5. Conclusions

In this study, we employed the SPEI to analyze the spatiotemporal characteristics of meteorological drought and wetness events in the coastal Savannah agroecological zone of Ghana from 1981 to 2021. Our findings support previous scientific evidence regarding the increased frequency and intensity of drought and wetness events.

The changepoint analysis revealed a more homogeneous nature of temperature and rainfall over the entire zone, except for September 1995 and November 2002, when changepoints occurred. The monthly variations revealed that drought and wetness event incidences follow the seasonal pattern of temperature and rainfall in the zone.

The temporal scale showed more moderate-to-extreme drought events in the 1980s and 1990s than in the 2000s, while the opposite is true for wetness events under both the SPEI-3 and SPEI-12 timescales. On the spatial scale, more extreme drought and wetness events occurred in the Central and Greater Accra areas, with severe conditions in the Volta areas. The SPEI-3 outperformed the SPEI-12 in extreme and severe drought and wetness event occurrences, indicating consequences for agriculture during the crop-growing season. Therefore, there is a need for the regular monitoring of drought and wet events to safeguard agricultural activities, especially those of smallholder farmers in the zone, in order to protect their livelihoods.

Supplementary Materials: The following supporting information can be downloaded at: https://www.mdpi.com/article/10.3390/w15010211/s1, Figure S1: Changepoints in temperature and rainfall for the coastal Savannah agroecological zone of Ghana; Figure S2: Temporal evolution of the mean annual SPEI-3 and SPEI-12 for moderate-to-extreme drought and wet events for the individual locations from 1981–2021 in the coastal Savannah agroecological zone in Ghana; Table S1: Changepoint analysis for climatic variables.

Author Contributions: Conceptualization: J.A.; Methodology: J.A.; Formal analysis and investigation: J.A.; Writing—original draft preparation: J.A.; Writing—review and editing: J.A., A.M. and

H.M.; Supervision: A.M. and H.M. All authors have read and agreed to the published version of the manuscript.

Funding: This research received no external funding.

Institutional Review Board Statement: Not applicable.

Informed Consent Statement: Not applicable.

Data Availability Statement: Not applicable.

Acknowledgments: This study is part of the Ph.D. research project 'Assessing climate change and climate variability impacts in the coastal savannah agroecological zone of Ghana' and Johnson Ankrah acknowledges the support of the Portuguese Foundation for Science and Technology (Fundação para a Ciência e Tecnologia)-FCT under the Ph.D. research scholarship (reference: 2021.05220.BD).

Conflicts of Interest: The authors declare no conflict of interest.

References

1. Liu, C.; Yang, C.; Yang, Q.; Wang, J. Spatiotemporal drought analysis by the standardized precipitation index (SPI) and standardized precipitation evapotranspiration index (SPEI) in Sichuan Province, China. *Sci. Rep.* **2021**, *11*, 1280. [CrossRef] [PubMed]
2. Cook, B.I.; Smerdon, J.E.; Seager, R.; Cook, E.R. Pan-Continental Droughts in North America over the Last Millennium. *J. Clim.* **2014**, *27*, 383–397. [CrossRef]
3. Dai, A. Characteristics and trends in various forms of the Palmer Drought Severity Index during 1900–2008. *J. Geophys. Res. Atmos.* **2011**, *116*, 4100509. [CrossRef]
4. Dai, A. The influence of the inter-decadal Pacific oscillation on US precipitation during 1923–2010. *Clim. Dyn.* **2013**, *41*, 633–646. [CrossRef]
5. Li, B.; Su, H.; Chen, F.; Wu, J.; Qi, J. The changing characteristics of drought in China from 1982 to 2005. *Nat. Hazards* **2013**, *68*, 723–743. [CrossRef]
6. Spinoni, J.; Naumann, G.; Carrao, H.; Barbosa, P.; Vogt, J. World drought frequency, duration, and severity for 1951–2010. *Int. J. Climatol.* **2014**, *34*, 2792–2804. [CrossRef]
7. Wilhite, D.A. *Drought and Water Crises: Science, Technology, and Management Issues*; CRC Press: Boca Raton, FL, USA, 2005. [CrossRef]
8. Zuo, D.; Cai, S.; Xu, Z.; Peng, D.; Kan, G.; Sun, W.; Pang, B.; Yang, H. Assessment of meteorological and agricultural droughts using in-situ observations and remote sensing data. *Agric. Water Manag.* **2019**, *222*, 125–138. [CrossRef]
9. EM-DAT: The CRED/OFDA International Disaster Database, Université Catholique de Louvain, Brussels, Belgium. Available online: https://www.emdat.be/ (accessed on 15 August 2022).
10. Capacity Development for Hazard Risk Reduction and Adaptation (CATALYST). Before Disaster Strikes: Transformation in Practice and Policy. (n.d). Available online: https://twas.org/sites/default/files/bpp_ewa_cs.pdf (accessed on 15 August 2022).
11. Wilhelmi, O.V.; Wilhite, D.A. Assessing vulnerability to agricultural drought: A Nebraska case study. *Nat. Hazards* **2002**, *25*, 37–58. [CrossRef]
12. Heim, R.R. A review of twentieth-century drought indices used in the United States. *Bull. Am. Meteorol. Soc.* **2002**, *83*, 1149–1166. [CrossRef]
13. Kogan, F.N. Droughts of the late 1980s in the United States as derived from NOAA polar-orbiting satellite data. *Bull. Am. Meteorol. Soc.* **1995**, *76*, 655–668. [CrossRef]
14. Alley, W.M. The Palmer drought severity index: Limitations and assumptions. *J. Appl. Meteorol. Climatol.* **1984**, *23*, 1100–1109. [CrossRef]
15. Vicente-Serrano, S.M.; Beguería, S.; López-Moreno, J.I. A multiscalar drought index sensitive to global warming: The standardized precipitation evapotranspiration index. *J. Clim.* **2010**, *23*, 1696–1718. [CrossRef]
16. McKee, T.B.; Doesken, N.J.; Kleist, J. The relationship of drought frequency and duration to time scales. In Proceedings of the 8th Conference on Applied Climatology, Anaheim, CA, USA, 17–22 January 1993; Volume 17, pp. 179–183.
17. Wilhite, D.A.; Glantz, M.H. Understanding: The drought phenomenon: The role of definitions. *Water Int.* **1985**, *10*, 111–120. [CrossRef]
18. Dracup, J.A.; Lee, K.S.; Paulson, E.G., Jr. On the definition of droughts. *Water Resour. Res.* **1980**, *16*, 297–302. [CrossRef]
19. Mishra, A.K.; Singh, V.P. A review of drought concepts. *J. Hydrol.* **2010**, *391*, 202–216. [CrossRef]
20. Tran, T.V.; Tran, D.X.; Myint, S.W.; Latorre-Carmona, P.; Ho, D.D.; Tran, P.H.; Dao, H.N. Assessing spatiotemporal drought dynamics and its related environmental issues in the Mekong River Delta. *Remote Sens.* **2019**, *11*, 2742. [CrossRef]
21. Palmer, W.C. *Meteorological Drought Research Paper No. 45*; Weather Bureau: Washington, DC, USA, 1965.
22. Nakalembe, C. Characterizing agricultural drought in the Karamoja subregion of Uganda with meteorological and satellite-based indices. *Nat. Hazards* **2018**, *91*, 837–862. [CrossRef]

23. Wang, Y.; Liu, G.; Guo, E. Spatial distribution and temporal variation of drought in Inner Mongolia during 1901–2014 using Standardized Precipitation Evapotranspiration Index. *Sci. Total Environ.* **2019**, *654*, 850–862. [CrossRef]
24. Zhang, A.; Jia, G. Monitoring meteorological drought in semiarid regions using multi-sensor microwave remote sensing data. *Remote Sens. Environ.* **2013**, *134*, 12–23. [CrossRef]
25. Wang, X.; Zhuo, L.; Li, C.; Engel, B.A.; Sun, S.; Wang, Y. Temporal and spatial evolution trends of drought in northern Shaanxi of China: 1960–2100. *Theor. Appl. Climatol.* **2020**, *139*, 965–979. [CrossRef]
26. Vicente-Serrano, S.M.; Beguería, S.; Lorenzo-Lacruz, J.; Camarero, J.J.; López-Moreno, J.I.; Azorin-Molina, C.; Revuelto, J.; Morán-Tejeda, E.; Sanchez-Lorenzo, A. Performance of drought indices for ecological, agricultural, and hydrological applications. *Earth Interact.* **2012**, *16*, 1–27. [CrossRef]
27. Quiring, S.M.; Ganesh, S. Evaluating the utility of the Vegetation Condition Index (VCI) for monitoring meteorological drought in Texas. *Agric. For. Meteorol.* **2010**, *150*, 330–339. [CrossRef]
28. Guttman, N.B.; Wallis, J.R.; Hosking, J.R.M. Spatial comparability of the palmer drought severity index. *JAWRA J. Am. Water Resour. Assoc.* **1992**, *28*, 1111–1119. [CrossRef]
29. Zhao, X.; Wu, P. Meteorological drought over the Chinese Loess Plateau: 1971–2010. *Nat. Hazards* **2013**, *67*, 951–961. [CrossRef]
30. Guttman, N.B. Accepting the standardized precipitation index: A calculation algorithm. *JAWRA J. Am. Water Resour. Assoc.* **1999**, *35*, 311–322. [CrossRef]
31. Liu, Z.; Wang, Y.; Shao, M.; Jia, X.; Li, X. Spatiotemporal analysis of multiscalar drought characteristics across the Loess Plateau of China. *J. Hydrol.* **2016**, *534*, 281–299. [CrossRef]
32. Minea, I.; Iosub, M.; Boicu, D. Multi-scale approach for different type of drought in temperate climatic conditions. *Nat. Hazards* **2022**, *110*, 1153–1177. [CrossRef]
33. Mishra, A.K.; Singh, V.P.; Desai, V.R. Drought characterization: A probabilistic approach. *Stoch. Environ. Res. Risk Assess.* **2009**, *23*, 41–55. [CrossRef]
34. Pei, Z.; Fang, S.; Wang, L.; Yang, W. Comparative analysis of drought indicated by the SPI and SPEI at various timescales in inner Mongolia, China. *Water* **2020**, *12*, 1925. [CrossRef]
35. Chen, Q.; Timmermans, J.; Wen, W.; van Bodegom, P.M. A multi-metric assessment of drought vulnerability across different vegetation types using high resolution remote sensing. *Sci. Total Environ.* **2022**, *832*, 154970. [CrossRef]
36. Paulo, A.A.; Rosa, R.D.; Pereira, L.S. Climate trends and behaviour of drought indices based on precipitation and evapotranspiration in Portugal. *Nat. Hazards Earth Syst. Sci.* **2012**, *12*, 1481–1491. [CrossRef]
37. Stagge, J.H.; Tallaksen, L.M.; Gudmundsson, L.; Van Loon, A.F.; Stahl, K. Candidate distributions for climatological drought indices (SPI and SPEI). *Int. J. Climatol.* **2015**, *35*, 4027–4040. [CrossRef]
38. Zhao, J.; Liu, Q.; Lu, H.; Wang, Z.; Zhang, K.; Wang, P. Future droughts in China using the standardized precipitation evapotranspiration index (SPEI) under multi-spatial scales. *Nat. Hazards* **2021**, *109*, 615–636. [CrossRef]
39. Liu, X.; Zhu, X.; Pan, Y.; Li, S.; Liu, Y.; Ma, Y. Agricultural drought monitoring: Progress, challenges, and prospects. *J. Geogr. Sci.* **2016**, *26*, 750–767. [CrossRef]
40. Gao, B. NDWI—A normalized difference water index for remote sensing of vegetation liquid water from space. *Remote Sens. Env.* **1996**, *266*, 257–266. [CrossRef]
41. IPCC. *Climate Change 2014: Synthesis Report*; Contribution of Working Groups I, II and III to the Fifth Assessment Report of the Intergovernmental Panel on Climate Change; Pachauri, R.K., Meyer, L.A., Eds.; IPCC: Geneva, Switzerland, 2014; p. 151.
42. Sheffield, J.; Wood, E.F.; Roderick, M.L. Little change in global drought over the past 60 years. *Nature* **2012**, *491*, 435–438. [CrossRef]
43. Wang, G.; Gong, T.; Lu, J.; Lou, D.; Hagan, D.F.T.; Chen, T. On the long-term changes of drought over China (1948–2012) from different methods of potential evapotranspiration estimations. *Int. J. Climatol.* **2018**, *38*, 2954–2966. [CrossRef]
44. Wilhite, D.A. Chapter 1 drought as a natural hazard: Concepts and definitions. In *Drought Mitigation Center Faculty Publications*; Routledge: London, UK, 2000; p. 69.
45. World Meteorological Organization. Experts Recommend Agricultural Drought Indices for improved understanding of food production conditions. In *Developments in Earth Surface Processes*; WMO: Murcia, Spain, 2010.
46. Trenberth, K.E.; Dai, A.; Van Der Schrier, G.; Jones, P.D.; Barichivich, J.; Briffa, K.R.; Sheffield, J. Global warming and changes in drought. *Nat. Clim. Change* **2014**, *4*, 17–22. [CrossRef]
47. Ayugi, B.; Tan, G.; Rouyun, N.; Zeyao, D.; Ojara, M.; Mumo, L.; Babaousmail, H.; Ongoma, V. Evaluation of meteorological drought and flood scenarios over Kenya, East Africa. *Atmosphere* **2020**, *11*, 307. [CrossRef]
48. Haile, G.G.; Tang, Q.; Leng, G.; Jia, G.; Wang, J.; Cai, D.; Sun, S.; Baniya, B.; Zhang, Q. Long-term spatiotemporal variation of drought patterns over the Greater Horn of Africa. *Sci. Total Environ.* **2020**, *704*, 135299. [CrossRef]
49. Okpara, J.N.; Afiesimama, E.A.; Anuforom, A.C.; Owino, A.; Ogunjobi, K.O. The applicability of Standardized Precipitation Index: Drought characterization for early warning system and weather index insurance in West Africa. *Nat. Hazards* **2017**, *89*, 555–583. [CrossRef]
50. Guo, H.; Bao, A.; Liu, T.; Jiapaer, G.; Ndayisaba, F.; Jiang, L.; Kurban, A.; De Maeyer, P. Spatial and temporal characteristics of droughts in Central Asia during 1966–2015. *Sci. Total Environ.* **2018**, *624*, 1523–1538. [CrossRef] [PubMed]
51. Miyan, M.A. Droughts in Asian least developed countries: Vulnerability and sustainability. *Weather Clim. Extrem.* **2015**, *7*, 8–23. [CrossRef]

52. Wang, L.; Chen, W.; Fu, Q.; Huang, G.; Wang, Q.; Chotamonsak, C.; Limsakul, A. Super droughts over East Asia since 1960 under the impacts of global warming and decadal variability. *Int. J. Climatol.* **2021**, *42*, 4508–4521. [CrossRef]
53. Deo, R.C.; Byun, H.R.; Adamowski, J.F.; Begum, K. Application of effective drought index for quantification of meteorological drought events: A case study in Australia. *Theor. Appl. Climatol.* **2017**, *128*, 359–379. [CrossRef]
54. Hoque, M.A.A.; Pradhan, B.; Ahmed, N.; Sohel, M.S.I. Agricultural drought risk assessment of Northern New South Wales, Australia using geospatial techniques. *Sci. Total Environ.* **2021**, *756*, 143600. [CrossRef]
55. Rahmat, S.N.; Jayasuriya, N.; Bhuiyan, M. Assessing droughts using meteorological drought indices in Victoria, Australia. *Hydrol. Res.* **2015**, *46*, 463–476. [CrossRef]
56. Lehner, B.; Döll, P.; Alcamo, J.; Henrichs, T.; Kaspar, F. Estimating the impact of global change on flood and drought risks in Europe: A continental, integrated analysis. *Clim. Change* **2006**, *75*, 273–299. [CrossRef]
57. Naumann, G.; Cammalleri, C.; Mentaschi, L.; Feyen, L. Increased economic drought impacts in Europe with anthropogenic warming. *Nat. Clim. Change* **2021**, *11*, 485–491. [CrossRef]
58. Cook, E.R.; Seager, R.; Cane, M.A.; Stahle, D.W. North American drought: Reconstructions, causes, and consequences. *Earth-Sci. Rev.* **2007**, *81*, 93–134. [CrossRef]
59. Shrestha, R.R.; Bonsal, B.R.; Bonnyman, J.M.; Cannon, A.J.; Najafi, M.R. Heterogeneous snowpack response and snow drought occurrence across river basins of northwestern North America under 1.0 °C to 4.0 °C global warming. *Clim. Change* **2021**, *164*, 40. [CrossRef]
60. Junqueira, R.; Amorim, J.da.S.; Viola, M.R.; Mello, C.R.d.; Uddameri, V.; Prado, L.F. Drought occurrences and impacts on the upper Grande river basin, Brazil. *Meteorol. Atmos. Phys.* **2022**, *134*, 45. [CrossRef]
61. Marengo, J.A.; Torres, R.R.; Alves, L.M. Drought in Northeast Brazil—Past, present, and future. *Theor. Appl. Climatol.* **2017**, *129*, 1189–1200. [CrossRef]
62. Rivera, J.A.; Penalba, O.C. Spatio-temporal assessment of streamflow droughts over Southern South America: 1961–2006. *Theor. Appl. Climatol.* **2018**, *133*, 1021–1033. [CrossRef]
63. Burke, E.J.; Brown, S.J.; Christidis, N. Modelling the recent evolution of global drought and projections for the twenty-first century with the Hadley Centre climate model. *J. Hydrometeorol.* **2006**, *7*, 1113–1125. [CrossRef]
64. Kogan, F.N. Global Drought Watch from Space. *Bull. Am. Meteorol. Soc.* **1997**, *78*, 621–636. [CrossRef]
65. Wang, T.; Tu, X.; Singh, V.P.; Chen, X.; Lin, K. Global data assessment and analysis of drought characteristics based on CMIP6. *J. Hydrol.* **2021**, *596*, 126091. [CrossRef]
66. Thiaw, W.M.; Kumar, V.B. NOAA'S African Desk: Twenty years of developing capacity in weather and climate forecasting in Africa. *Bull. Am. Meteorol. Soc.* **2015**, *96*, 737–753. [CrossRef]
67. Okpara, J.N.; Tarhule, A.; Perumal, M. Study of climate change in Niger River Basin, West Africa: Reality not a myth. In *Climate Change - Realities Impacts Over Ice Cap Sea Level Risks*; InTech: London, UK, 2013; Volume 1, pp. 3–38. [CrossRef]
68. Dei, G.J. Coping with the effects of the 1982–83 drought in Ghana: The view from the village. *Afr. Dev. Afr. Développement* **1988**, *13*, 107–122.
69. Antwi-Agyei, P.; Fraser, E.D.G.; Dougill, A.J.; Stringer, L.C.; Simelton, E. Mapping the vulnerability of crop production to drought in Ghana using rainfall, yield and socioeconomic data. *Appl. Geogr.* **2012**, *32*, 324–334. [CrossRef]
70. Dumenu, W.K.; Obeng, E.A. Climate change and rural communities in Ghana: Social vulnerability, impacts, adaptations and policy implications. *Environ. Sci. Policy* **2016**, *55*, 208–217. [CrossRef]
71. Kasei, R.; Diekkrüger, B.; Leemhuis, C. Drought frequency in the Volta Basin of West Africa. *Sustain. Sci.* **2010**, *5*, 89–97. [CrossRef]
72. Ndehedehe, C.E.; Awange, J.L.; Corner, R.J.; Kuhn, M.; Okwuashi, O. On the potentials of multiple climate variables in assessing the spatio-temporal characteristics of hydrological droughts over the Volta Basin. *Sci. Total Environ.* **2016**, *557–558*, 819–837. [CrossRef] [PubMed]
73. Nyatuame, M.; Agodzo, S. Analysis of Extreme Rainfall Events (Drought and Flood) over Tordzie Watershed in the Volta Region of Ghana. *J. Geosci. Environ. Prot.* **2017**, *5*, 275–295. [CrossRef]
74. Oguntunde, P.G.; Abiodun, B.J.; Lischeid, G. Impacts of climate change on hydro-meteorological drought over the Volta Basin, West Africa. *Glob. Planet. Change* **2017**, *155*, 121–132. [CrossRef]
75. Dovie, D.B.K.; Kasei, R.A. Hydro-climatic stress, shallow groundwater wells and coping in Ghana's White Volta basin. *Sci. Total Environ.* **2018**, *636*, 1268–1278. [CrossRef]
76. Akurugu, B.A.; Obuobie, E.; Yidana, S.M.; Stisen, S.; Seidenfaden, I.K.; Chegbeleh, L.P. Groundwater resources assessment in the Densu Basin: A review. *J. Hydrol. Reg. Stud.* **2022**, *40*, 101017. [CrossRef]
77. Nasirudeen, A.F.; Kabo-bah, A.T.; Amo-Boateng, M.; Karthikeyan, B. Analysis of drought patterns in the Tano river basin of Ghana. *Sci. Afr.* **2021**, *13*, e00883. [CrossRef]
78. Addi, M.; Asare, K.; Fosuhene, S.K.; Ansah-Narh, T.; Aidoo, K.; Botchway, C.G. Impact of Large-Scale Climate Indices on Meteorological Drought of Coastal Ghana. *Adv. Meteorol.* **2021**, *2021*, 8899645. [CrossRef]
79. Asare-Nuamah, P.; Botchway, E. Understanding climate variability and change: Analysis of temperature and rainfall across agroecological zones in Ghana. *Heliyon* **2019**, *5*, e02654. [CrossRef]
80. Bessah, E.; Amponsah, W.; Ansah, S.O.; Afrifa, A.; Yahaya, B.; Wemegah, C.S.; Tanu, M.; Amekudzi, L.K.; Agyare, W.A. Climatic zoning of Ghana using selected meteorological variables for the period 1976–2018. *Meteorol. Appl.* **2022**, *29*, 1–15. [CrossRef]

81. Gbangou, T.; Ludwig, F.; van Slobbe, E.; Greuell, W.; Kranjac-Berisavljevic, G. Rainfall and dry spell occurrence in Ghana: Trends and seasonal predictions with a dynamical and a statistical model. *Appl. Climatol.* **2020**, *141*, 371–387. [CrossRef]
82. Baidu, M.; Amekudzi, L.K.; Aryee, J.N.A.; Annor, T. Assessment of Long-Term Spatio-Temporal Rainfall Variability over Ghana using Wavelet Analysis. *Climate* **2017**, *5*, 30. [CrossRef]
83. Ghana Statistical Service. *2010 Population and Housing Census*; National Analytical Report; Ghana Statistical Service: Accra, Ghana, 2013; p. 430. Available online: https://statsghana.gov.gh/gssmain/fileUpload/pressrelease/2010_PHC_National_Analytical_Report.pdf (accessed on 16 November 2022).
84. Dickson, K.B.; Benneh, G. *A New Geography of Ghana, Revised Edition*; Longman Group Ltd.: London, UK, 2001.
85. NASA Prediction of Worldwide Energy Resources. The Power Project. (n.d). Available online: https://power.larc.nasa.gov/ (accessed on 7 June 2022).
86. Monteiro, L.A.; Sentelhas, P.C.; Pedra, G.U. Assessment of NASA/POWER satellite-based weather system for Brazilian conditions and its impact on sugarcane yield simulation. *Int. J. Climatol.* **2018**, *38*, 1571–1581. [CrossRef]
87. Marzouk, O.A. Assessment of global warming in Al Buraimi, sultanate of Oman based on statistical analysis of NASA POWER data over 39 years, and testing the reliability of NASA POWER against meteorological measurements. *Heliyon* **2021**, *7*, e06625. [CrossRef]
88. Mourtzinis, S.; Edreira, J.I.R.; Conley, S.P.; Grassini, P. From grid to field: Assessing quality of gridded weather data for agricultural applications. *Eur. J. Agron.* **2017**, *82*, 163–172. [CrossRef]
89. R-Instat. Version 0.70. Available online: http://r-instat.org/About.html (accessed on 7 June 2022).
90. Pettitt, A.N. A non-parametric approach to the change-point problem. *J. R. Stat. Society. Ser. C (Appl. Stat.)* **1979**, *28*, 126–135. [CrossRef]
91. Buishand, T.A. Some methods for testing the homogeneity of rainfall records. *J. Hydrol.* **1982**, *58*, 11–27. [CrossRef]
92. Alexandersson, H.A. Homogeneity test applied to precipitation data. *J. Climatol.* **1986**, *6*, 661–675. [CrossRef]
93. Wijngaard, J.B.; Klein Tank, A.M.G.; Können, G.P. Homogeneity of 20th century European daily temperature and precipitation series. *Int. J. Climatol.* **2003**, *23*, 679–692. [CrossRef]
94. Yildirim, G.; Rahman, A. Homogeneity and trend analysis of rainfall and droughts over Southeast Australia. *Nat. Hazards* **2022**, *112*, 1657–1683. [CrossRef]
95. Jaiswal, R.K.; Lohani, A.K.; Tiwari, H.L. Statistical analysis for change detection and trend assessment in climatological parameters. *Environ. Process.* **2015**, *2*, 729–749. [CrossRef]
96. Hargreaves, G.L.; Samani, Z.A. Reference crop evapotranspiration from temperature. *Appl. Eng. Agric.* **1985**, *1*, 96–99. [CrossRef]
97. Beguería, S.; Vicente-Serrano, S.M.; Reig, F.; Latorre, B. Standardized precipitation evapotranspiration index (SPEI) revisited: Parameter fitting, evapotranspiration models, tools, datasets and drought monitoring. *Int. J. Climatol.* **2014**, *34*, 3001–3023. [CrossRef]
98. Gozzo, L.F.; Palma, D.S.; Custodio, M.S.; Machado, J.P. Climatology and trend of severe drought events in the state of Sao Paulo, Brazil, during the 20th Century. *Atmosphere* **2019**, *10*, 190. [CrossRef]
99. Polong, F.; Chen, H.; Sun, S.; Ongoma, V. Temporal and spatial evolution of the standard precipitation evapotranspiration index (SPEI) in the Tana River Basin, Kenya. *Appl. Climatol.* **2019**, *138*, 777–792. [CrossRef]
100. Mann, H.B. Nonparametric tests against trend. *Econometrica* **1945**, *13*, 245–259. [CrossRef]
101. Kendall, M.G. *Rank Correlation Methods*; Griffin: London, UK, 1975.
102. Da Silva, R.M.; Santos, C.A.G.; Moreira, M.; Corte-Real, J.; Silva, V.C.L.; Medeiros, I.C. Rainfall and river flow trends using Mann–Kendall and Sen's slope estimator statistical tests in the Cobres River basin. *Nat. Hazards* **2015**, *77*, 1205–1221. [CrossRef]
103. Zhang, H.; Ding, M.; Li, L.; Liu, L. Continuous Wetting on the Tibetan Plateau during 1970–2017. *Water* **2019**, *11*, 2605. [CrossRef]
104. Gocic, M.; Trajkovic, S. Analysis of changes in meteorological variables using Mann-Kendall and Sen's slope estimator statistical tests in Serbia. *Glob. Planet. Change* **2013**, *100*, 172–182. [CrossRef]
105. Sen, P.K. Estimates of the regression coefficient based on Kendall's tau. *J. Am. Stat. Assoc.* **1968**, *63*, 1379–1389. [CrossRef]
106. Shahid, S. Rainfall variability and the trends of wet and dry periods in Bangladesh. *Int. J. Climatol.* **2010**, *30*, 2299–2313. [CrossRef]
107. Mustafa, A.; Rahman, G. Assessing the spatio-temporal variability of meteorological drought in Jordan. *Earth Syst. Env.* **2018**, *2*, 247–264. [CrossRef]
108. Sun, Y.; Liu, S.; Dong, Y.; Dong, S.; Shi, F. Effects of multi-time scales drought on vegetation dynamics in Qaidam River Basin, Qinghai-Tibet Plateau from 1998 to 2015. *Appl. Climatol.* **2020**, *141*, 117–131. [CrossRef]
109. Dai, A. Future warming patterns linked to today's climate variability. *Sci. Rep.* **2016**, *6*, 19110. [CrossRef]
110. Lyon, B. Seasonal Drought in the Greater Horn of Africa and its recent increase during the March–May long rains. *J. Clim.* **2014**, *27*, 7953–7975. [CrossRef]
111. García-Marín, A.P.; Estévez, J.; Morbidelli, R.; Saltalippi, C.; Ayuso-Muñoz, J.L.; Flammini, A. Assessing inhomogeneities in extreme annual rainfall data series by multifractal approach. *Water* **2020**, *12*, 1030. [CrossRef]
112. Wang, F.; Wang, Z.; Yang, H.; Zhao, Y. Study of the temporal and spatial patterns of drought in the Yellow River basin based on SPEI. *Sci. China Earth Sci.* **2018**, *61*, 1098–1111. [CrossRef]
113. An, Q.; He, H.; Nie, Q.; Cui, Y.; Gao, J.; Wei, C.; Xie, X.; You, J. Spatial and temporal variations of drought in Inner Mongolia, China. *Water* **2020**, *12*, 1715. [CrossRef]

114. Ge, Y.; Cai, X.; Zhu, T.; Ringler, C. Drought frequency change: An assessment in northern India plains. *Agric. Water Manag.* **2016**, *176*, 111–121. [CrossRef]
115. Alsafadi, K.; Mohammed, S.A.; Ayugi, B.; Sharaf, M.; Harsányi, E. Spatial–temporal evolution of drought characteristics over Hungary between 1961 and 2010. *Pure Appl. Geophys.* **2020**, *177*, 3961–3978. [CrossRef]
116. Asante, F.; Amuakwa-Mensah, F. Climate Change and Variability in Ghana: Stocktaking. *Climate* **2015**, *3*, 78–99. [CrossRef]
117. Ahmed, S.M. Impacts of drought, food security policy and climate change on performance of irrigation schemes in Sub-Saharan Africa: The case of Sudan. *Agric. Water Manag.* **2020**, *232*, 106064. [CrossRef]
118. Daryanto, S.; Wang, L.; Jacinthe, P.-A. Global synthesis of drought effects on maize and wheat Production. *PLoS ONE* **2016**, *11*, e0156362. [CrossRef]
119. Gautier, D.; Denis, D.; Locatelli, B. Impacts of drought and responses of rural populations in West Africa: A systematic review. *WIREs Clim. Change* **2016**, *7*, 666–681. [CrossRef]
120. Leng, G.; Hall, J. Crop yield sensitivity of global major agricultural countries to droughts and the projected changes in the future. *Sci. Total Environ.* **2019**, *654*, 811–821. [CrossRef]
121. Li, Q.; Cao, Y.; Miao, S.; Huang, X. Spatiotemporal characteristics of drought and wet events and their impacts on agriculture in the Yellow River Basin. *Land* **2022**, *11*, 556. [CrossRef]
122. Wang, C.; Linderholm, H.W.; Song, Y.; Wang, F.; Liu, Y.; Tian, J.; Xu, J.; Song, Y.; Ren, G. Impacts of drought on maize and soybean production in northeast China during the past five decades. *Int. J. Environ. Res. Public Health* **2020**, *17*, 2459. [CrossRef]
123. Zipper, S.C.; Qiu, J.; Kucharik, C.J. Drought effects on US maize and soyabean production: Spatiotemporal patterns and historical changes. *Environ. Res. Lett.* **2016**, *11*, 094021. [CrossRef]
124. Yaro, J.A. The perception of and adaptation to climate variability/change in Ghana by small-scale and commercial farmers. *Reg. Env. Change* **2013**, *13*, 1259–1272. [CrossRef]
125. Manatsa, D.; Mukwada, G.; Siziba, E.; Chinyanganya, T. Analysis of multidimensional aspects of agricultural droughts in Zimbabwe using the Standardized Precipitation Index (SPI). *Appl. Climatol.* **2010**, *102*, 287–305. [CrossRef]
126. Santos, J.F.; Pulido-Calvo, I.; Portela, M.M. Spatial and temporal variability of droughts in Portugal. *Water Resour. Res.* **2010**, *46*, W03503. [CrossRef]
127. Zhao, G.; Mu, X.; Hörmann, G.; Fohrer, N.; Xiong, M.; Su, B.; Li, X. Spatial patterns and temporal variability of dryness/wetness in the Yangtze River Basin, China. *Quat. Int.* **2012**, *282*, 5–13. [CrossRef]
128. Chiang, F.; Mazdiyasni, O.; AghaKouchak, A. Evidence of anthropogenic impacts on global drought frequency, duration, and intensity. *Nat. Commun.* **2021**, *12*, 2754. [CrossRef]
129. Brito, S.S.B.; Cunha, A.P.M.A.; Cunningham, C.C.; Alvalá, R.C.; Marengo, J.A.; Carvalho, M.A. Frequency, duration and severity of drought in the Semiarid Northeast Brazil region. *Int. J. Clim.* **2018**, *38*, 517–529. [CrossRef]
130. Christidis, N.; Stott, P.A. The influence of anthropogenic climate change on wet and dry summers in Europe. *Sci. Bull.* **2011**, *66*, 813–823. [CrossRef]
131. Kastridis, A.; Kamperidou, V.; Stathis, D. Dendroclimatological analysis of Fir (*A. borisii-regis*) in Greece in the frame of climate change investigation. *Forests* **2022**, *13*, 879. [CrossRef]
132. Mersin, D.; Tayfur, G.; Vaheddoost, B.; Safari, M.J.S. Historical trends associated with annual temperature and precipitation in Aegean Turkey, where are we heading? *Sustainability* **2022**, *14*, 13380. [CrossRef]
133. Todaro, V.; D'Oria, M.; Secci, D.; Zanini, A.; Tanda, M.G. Climate change over the Mediterranean region: Local temperature and precipitation variations at five pilot sites. *Water* **2022**, *14*, 2499. [CrossRef]
134. Swain, S.; Hayhoe, K. CMIP5 projected changes in spring and summer drought and wet conditions over North America. *Clim. Dyn.* **2015**, *44*, 2737–2750. [CrossRef]
135. Sheffield, J.; Wood, E.F. Projected changes in drought occurrence under future global warming from multi-model, multi-scenario, IPCC AR4 simulations. *Clim. Dyn.* **2008**, *31*, 79–105. [CrossRef]
136. Elbeltagi, A.; AlThobiani, F.; Kamruzzaman, M.; Shaid, S.; Roy, D.K.; Deb, L.; Islam, M.M.; Kundu, P.K.; Rahman, M.M. Estimating the standardized precipitation evapotranspiration index using data-driven techniques: A regional study of Bangladesh. *Water* **2022**, *14*, 1764. [CrossRef]
137. Kuntiyawichai, K.; Wongsasri, S. Assessment of drought severity and vulnerability in the Lam Phaniang river basin, Thailand. *Water* **2021**, *13*, 2743. [CrossRef]